International Ocean Discovery Program Expedition 401 Scientific Prospectus

Mediterranean–Atlantic Gateway Exchange

Rachel Flecker
Co-Chief Scientist
School of Geographical Sciences
University of Bristol
UK

Emmanuelle Ducassou
Co-Chief Scientist
UMR Environnements Paléoenvironnements Océaniques et Continentaux
Université de Bordeaux
France

Trevor Williams
Expedition Project Manager/Staff Scientist
International Ocean Discovery Program
Texas A&M University
USA

Publisher's notes

This publication was prepared by the *JOIDES Resolution* Science Operator (JRSO) at Texas A&M University (TAMU) as an account of work performed under the International Ocean Discovery Program (IODP). This material is based upon work supported by the JRSO, which is a major facility funded by the National Science Foundation Cooperative Agreement Number OCE1326927. Funding for IODP is provided by the following international partners:

National Science Foundation (NSF), United States
Ministry of Education, Culture, Sports, Science and Technology (MEXT), Japan
European Consortium for Ocean Research Drilling (ECORD)
Ministry of Science and Technology (MOST), People's Republic of China
Australia-New Zealand IODP Consortium (ANZIC)
Ministry of Earth Sciences (MoES), India

Portions of this work may have been published in whole or in part in other IODP documents or publications.

This IODP *Scientific Prospectus* is based on precruise *JOIDES Resolution* Facility advisory panel discussions and scientific input from the designated Co-Chief Scientists on behalf of the drilling proponents. During the course of the cruise, actual site operations may indicate to the Co-Chief Scientists, the Expedition Project Manager/Staff Scientist, and the Operations Superintendent that it would be scientifically or operationally advantageous to amend the plan detailed in this prospectus. It should be understood that any substantial changes to the science deliverables outlined in the plan presented here are contingent upon the approval of the IODP JRSO Director and/or *JOIDES Resolution* Facility Board.

Disclaimer

Copyright

Citation

Flecker, R., Ducassou, E., and Williams, T., 2023. Expedition 401 Scientific Prospectus: Mediterranean–Atlantic Gateway Exchange. International Ocean Discovery Program. https://doi.org/10.14379/iodp.sp.401.2023

ISSN

World Wide Web: 2332-1385

April 2023

Abstract

Marine gateways play a critical role in the exchange of water, heat, salt, and nutrients between oceans and seas. The advection of dense waters helps drive global thermohaline circulation, and because the ocean is the largest of the rapidly exchanging CO_2 reservoirs, this advection also affects atmospheric carbon concentration. Changes in gateway geometry can therefore significantly alter both the pattern of global ocean circulation and associated heat transport and climate, as well as having a profound local impact.

Today, the volume of dense water supplied by Atlantic–Mediterranean exchange through the Gibraltar Strait is amongst the largest in the global ocean. For the past 5 My, this overflow has generated a saline plume at intermediate depths in the Atlantic that deposits distinctive contouritic sediments in the Gulf of Cadiz and contributes to the formation of North Atlantic Deep Water. This single gateway configuration only developed in the early Pliocene, however. During the Miocene, a wide, open seaway linking the Mediterranean and Atlantic evolved into two narrow corridors: one in northern Morocco, the other in southern Spain. Formation of these corridors permitted Mediterranean salinity to rise and a new, distinct, dense water mass to form and overspill into the Atlantic for the first time. Further restriction and closure of these connections resulted in extreme salinity fluctuations in the Mediterranean, leading to the formation of the Messinian Salinity Crisis salt giant.

Investigating Miocene Mediterranean–Atlantic Gateway Exchange (IMMAGE) is an amphibious drilling proposal designed to recover a complete record of Atlantic–Mediterranean exchange from its Late Miocene inception to its current configuration. This will be achieved by targeting Miocene offshore sediments on either side of the Gibraltar Strait during International Ocean Discovery Program (IODP) Expedition 401 and recovering Miocene core from the two precursor connections now exposed on land with future International Continental Scientific Drilling Program (ICDP) campaigns. The scientific aims of IMMAGE are to constrain quantitatively the consequences for ocean circulation and global climate of the inception of Atlantic–Mediterranean exchange, to explore the mechanisms for high-amplitude environmental change in marginal marine systems, and to test physical oceanographic hypotheses for extreme high-density overflow dynamics that do not exist in the world today on this scale.

Plain language summary

Today, Mediterranean–Atlantic seawater exchange takes place exclusively through the Gibraltar Strait. Around 8 million years ago, however, there were another two gateways: one in northern Morocco and the other through southern Spain. Both connections have subsequently closed and been tectonically uplifted and preserved on land. This process contributed to a major episode of global cooling in at least two ways:

1. Initial restriction of seawater exchange through these marine corridors caused the saltiness of the Mediterranean to increase and generated a dense water body that flowed out into the Atlantic, changing the pattern of global ocean circulation and drawing CO_2 dissolved in surface waters down into deeper parts of the ocean.
2. Extreme restriction of the pre-Gibraltar Strait connections raised salinity in the Mediterranean substantially, leading to the precipitation of more than 1 km of salt on the Mediterranean Sea floor. This phenomenon, known as a salt giant, occurs episodically in Earth's history but no salt giant is forming today. The extraction of large volumes of salts from seawater changes ocean chemistry, which has knock-on consequences for the global carbon cycle and hence is a driver of climate change.

The chemical and physical properties of the sediments preserved in and on either side of the fossilized corridors are key to understanding and quantifying the global cooling caused by changes to Atlantic–Mediterranean exchange 5–8 million years ago. IODP Expedition 401 will recover records of exchange preserved offshore in the Atlantic and Mediterranean, and subsequent onshore drilling with ICDP will target the fossil gateway records that are now preserved on land in north-

ern Morocco and southern Spain. The Investigate the Miocene Mediterranean–Atlantic Gateway Exchange (IMMAGE) project is the first Land-2-Sea drilling project.

1. Schedule for Expedition 401

International Ocean Discovery Program (IODP) Expedition 401 is the offshore drilling component of the first Land-2-Sea drilling project, Investigating Miocene Mediterranean–Atlantic Gateway Exchange (IMMAGE), which also involves International Continental Scientific Drilling Program (ICDP) drilling onshore southern Spain and northern Morocco. Expedition 401 is based on IODP drilling proposal 895 (including versions 895-Full3 and 895-Add2, available at **http://iodp.tamu.edu/scienceops/expeditions/mediterranean_atlantic_gateway_exchange.html**). Following evaluation by the IODP Scientific Advisory Structure and Environmental Protection and Safety Panel (EPSP), the expedition was scheduled for the research vessel (R/V) *JOIDES Resolution*, operating under contract with the *JOIDES Resolution* Science Operator (JRSO). At the time of publication of this Scientific Prospectus, the expedition is scheduled to start in Amsterdam, The Netherlands, on 10 December 2023 and to end in Naples, Italy, on 9 February 2024. A total of 61 days will be available for the transit, drilling, coring, and downhole measurements described in this report (for the current detailed schedule, see **http://iodp.tamu.edu/scienceops**). Further details about the facilities aboard *JOIDES Resolution* can be found at **http://iodp.tamu.edu/labs/index.html**.

2. Background

Paleoclimate research is often driven by the need to validate various types of climate models under boundary conditions different from those of the last 150 y for which an instrumental record of climate is available (Intergovernmental Panel on Climate Change, 2014). Quantifying past changes in temperature, momentum, and flux in the ocean and atmosphere is therefore a key target for geological research. However, the small size of climate change signals relative to climate proxy measurement uncertainty means this is challenging to achieve (Rohling, 2007). A high signal to noise ratio typically requires amplification of the climate variable, and in the ocean, this is most commonly found in marginal marine basins where exchange with the open ocean is limited so it cannot buffer and diminish the signal of environmental change (Grant et al., 2017). Unfortunately, limited exchange also makes it difficult to use the enhanced marginal basin record to extrapolate to global-scale oceanographic change (Kaminski et al., 2002). Marine gateways linking the basin to the open ocean represent a sweet spot where on one side climatic changes are amplified in the adjoining marginal basin, whereas on the other, their impact on globally-meaningful changes in the open ocean can be directly assessed. In addition, the geometric and hydraulic restriction of the gateway itself places physical limitations on the freedom of the system to change (Nelson et al., 1999). This focuses the deposition of the sedimentological archive of exchange into a small, well-defined geographical area, making it possible to constrain quantitatively responses to exchange that impact global climate (Rogerson et al., 2012b).

The influence of exchanging heat, salt, and momentum through narrow, shallow straits that link the open ocean to marginal basins is profound. The advection of cool or saline waters (Legg et al., 2009) helps drive global thermohaline circulation (Thomas et al., 2004; Álvarez et al., 2005; Rahmstorf, 2006). Because the ocean is the largest of the rapidly exchanging CO_2 reservoirs, this advection also increases the sensitivity of the ocean to atmospheric carbon changes (LaRiviere et al., 2012; Karas et al., 2017; Elsworth et al., 2017; Capella et al., 2019). Although exchange through the Denmark Strait, Indonesian archipelago, and Gibraltar Strait can all overprint both zonal and meridional circulation patterns, global ocean surface circulation and associated heat transport compensating for water-mass transformation on the basinward side of gateways forces substantial impacts on sea ice and warming or cooling of adjacent continents and the position of the atmospheric front (Ivanovic et al., 2014a). Unsurprisingly, the opening and closure of oceanic gateways is therefore well recognized as having a profound impact on the Earth's climate, including its periodic switching from Greenhouse to Icehouse conditions (Kennett, 1982; Smith and Pickering, 2003; Knutz, 2008).

The impact of regional changes on global-scale processes are generally ideal questions for the Earth System Models theme. However, because of the inherent small-scale of marine gateways relative to global circulation model grid cells, the gateways are either hugely enlarged in the model or the transport of heat and water through them is parameterized rather than explicitly modeled (e.g., Dietrich et al., 2008; Ivanovic et al., 2013). An excellent example of the problem occurs at Gibraltar (Figure **F1**), where model grid cells of ~400 km^2, which are suitable for the long global simulations necessary for paleoclimate studies, are ill-equipped to simulate hydraulic control in a strait ~12 km in width and consequently generate exchange behavior which differs from observations (Ivanovic et al., 2013; Alhammoud et al., 2010). Consequently, the codependence of ocean and marginal sea in simulations is reduced, preconditioning models to be insensitive to exchange-driven change. A view of past and future climate derived from global circulation assessments alone therefore systematically underestimates the role of gateway processes, eliminating a crucial feedback within the Earth system.

In summary, exchange through marine gateways is an example of a key climate process that can only be constrained through interrogation of the record of ocean-marginal basin exchange in a specific sedimentary archive, and as a result is a target that fits precisely with the climate themes stated in the IODP and ICDP science plans.

2.1. Atlantic–Mediterranean exchange, now and in the past

In the Atlantic, several marine overflows (Denmark Strait, Mediterranean, and Weddell Sea) supply dense water that collectively feeds the thermohaline circulation system (Smethie et al., 2000). The transportation of dense water from the Mediterranean into the interior of the Atlantic (Figure **F1**) is amongst the largest in the global ocean (Legg et al., 2009) (Table **T1**), and exchange also provides a key exit point for Atlantic buoyancy, the underlying driver behind Atlantic deep convection (Broecker, 1991).

The dense Mediterranean overflow (MO) is generated as a consequence of its midlatitude setting where evaporation exceeds precipitation (Peixoto and Kettani, 1973), generating a warm, salty water mass. The negative hydrologic budget varies in severity through time, amplifying the climate signal transmitted principally through the Mediterranean's southern catchments and derived from North African monsoon rainfall (Marzocchi et al., 2015) (Figure **F1**). This subtropical monsoonal climate signal with its strong precessional pulse is then propagated into the Atlantic by density-driven exchange (Bahr et al., 2015) through the Gibraltar Strait. Water flowing out of the Mediterranean at depth entrains ambient Atlantic water as it goes (Dietrich et al., 2008), generating a distinctive Atlantic–Mediterranean Water (AMW) mass (Rogerson et al., 2012b) in the cen-

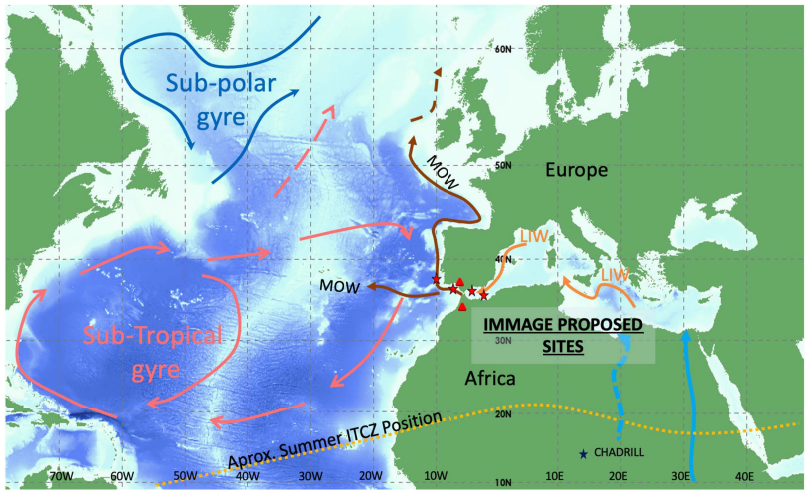

Figure F1. Climatic transport system linking the North African monsoonal system via MO to thermohaline circulation in the North Atlantic. Red stars are the proposed IODP IMMAGE sites; red triangles are the ICDP IMMAGE sites. Arrows indicate surface and intermediate water masses. AMW = Atlantic–Mediterranean Water, LIW = Levantine Intermediate Water, ITCZ = Intertropical Convergence Zone.

tral and north Atlantic and large depositional and erosional features including extensive sandy contouritic drifts (Nelson et al., 1999; Expedition 339 Scientists, 2013; Hernández-Molina et al., 2003, 2014a, 2014b). AMW flows north, fueling the Norwegian Sea with higher density water that helps sustain the formation and southward flow of North Atlantic Deep Water (NADW) (Khélifi et al., 2009; Rogerson et al., 2012b; Kaboth et al., 2018).

Despite the challenges of modeling the gateway, the exchange that occurs through the Gibraltar Strait today is a sufficiently influential component of the Earth System for general circulation models to capture at least part of its impact (Bigg et al., 2003; Bigg and Wadley, 2001). Experiments without Atlantic–Mediterranean exchange show that its presence makes Greenland warmer and Antarctica cooler (Bigg et al., 2003). This in turn is sufficient to shift the position of the Intertropical Convergence Zone (Figure **F1**), and hence the location of monsoons, storm tracks, and the hyper-arid zones between them. Atlantic–Mediterranean exchange is also a critical component of Atlantic Meridional Overturning Circulation (AMOC), particularly at times of weak NADW formation (Bigg and Wadley, 2001; Ivanovic et al., 2014a, 2014b; Penaud et al., 2011; Rogerson et al., 2006, 2010; Voelker et al., 2006). Furthermore, the transport of dense water from the Mediterranean into the interior of the Atlantic entrains ambient Atlantic water on route, contributing significantly to global carbon drawdown (2%–5% of today's total net ocean carbon sink; Tans et al., 1993; Siegenthaler and Sarmiento, 1993; Dixon et al., 1994). Taken altogether, this makes Atlantic–Mediterranean exchange a key teleconnection that links African monsoon precipitation derived from the south Atlantic with the northern high latitudes.

Exchange through a single gateway at Gibraltar is a relatively recent phenomenon (Hernández-Molina et al., 2014b; van der Schee et al., 2016; García-Gallardo et al., 2017a, 2017b). As a result of Africa-Eurasia convergence, westward docking of the Alborán plate and simultaneous slab-retreat (Jolivet and Faccenna, 2000; Faccenna et al., 2004; van Hinsbergen et al., 2014), the Atlantic–Mediterranean connection evolved from a single, wide open seaway (Figure **F2**; Table **T1**) linking a Mediterranean that was more of an embayment of the Atlantic than a distinct marginal marine

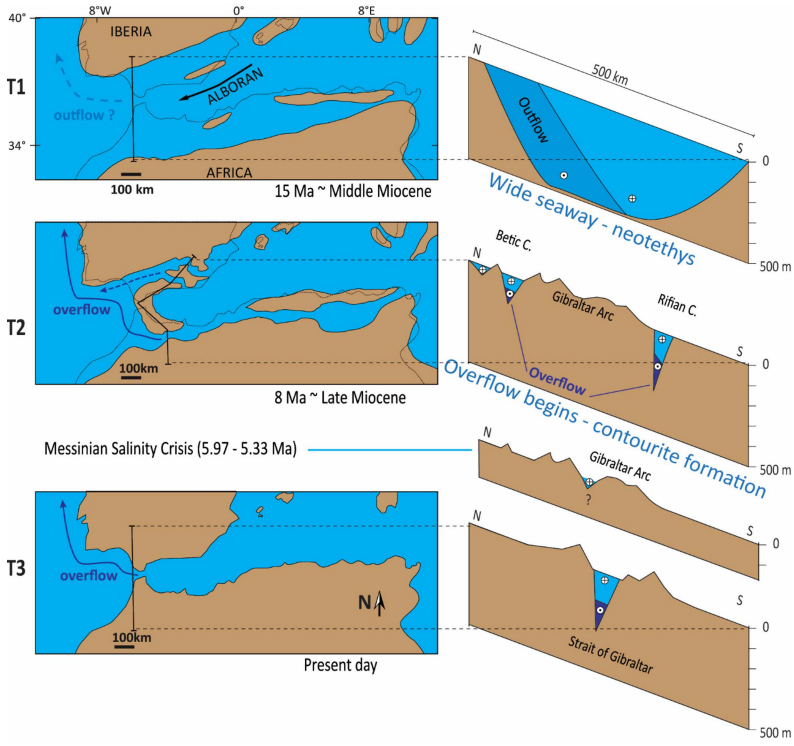

Figure F2. Tectonically-controlled reconfiguration of the Mediterranean–Atlantic seaways from Middle Miocene to present day. Paleogeography of the Western Mediterranean after Do Couto et al. (2016). The Rifian/Betic seaways (T2), which replaced a wider seaway (T1), are now exposed on land in northern Morocco and southern Spain. The T2 scenario (~8 Ma) is the first with potential impact on Atlantic–Mediterranean salinity gradients and overflow formation. (Figure from Capella et al., 2019.)

system (Flecker et al., 2015) to two narrow corridors: one in northern Morocco, the other in southern Spain (Benson et al., 1991) (Table T2). The onset of episodic organic-rich sedimentation (sapropels) in the Middle Miocene (Hilgen et al., 2005; Taylforth et al., 2014) is the earliest evidence of the Mediterranean operating separately from the Atlantic. Ongoing progressive restriction of the marine corridors permitted Mediterranean salinity to rise, and a distinct, dense water mass formed. This dense water overspill into the Atlantic for the first time at some point during the Middle–Late Miocene (Capella et al., 2017, 2019). Ultimately, the narrowing and closure of these connections resulted in extreme salinity fluctuations in the Mediterranean, leading to the precipitation of more than 1 million km^3 of salt, equivalent to ~6% of the total dissolved oceanic NaCl

Table T1. Data from several overflows for comparison with present day exchange through the Gibraltar Strait and estimated Late Miocene Atlantic–Mediterranean exchange. Data for the modern ocean is taken from Legg et al., (2009).

				Gibraltar Exchange		
	Faroe Bank	Denmark Strait	Red Sea	Today	Messinian Halite Phase	Lago Mare Phase
Source water						
Potential temperature	0	0.25	22.8	14	14	14
Salinity (g/kg)	34.92	34.1	39.8	38.4	360	36
Density at Surface (s units)	28.07	27.94	27.7	28.94	~300	~26.96
Sill depth (m)	800	500	200	300	20	200
Density difference at gateway (σ)	1.57	1.44	1.2	2.44	~275	~0.5
Product water						
Potential temperature	3.3	2.1	21.7	11.8	?	?
Salinity (g/kg)	35.1	34.84	34.67	36.4	?	?
Density at Surface (s units)	27.9	27.85	27.48	27.6	?	?
Depth (m)	3000	1600	750	850	?	?
Velocity Source (m/s)	1	0.7	0.55	1	≫1	≪1
Transport						
Source	1.8	2.9	0.3	0.8	≪0.8	?
Product (Sv)	3.3	5.2	0.55	2.3	~2.3	?
Entrainment %	183	179	183	288	≫288	?

Table T2. Operations plan and time estimates for primary sites, Expedition 401, Option 1 (see text). mbrf = meters below rig floor. EPSP = Environmental Protection and Safety Panel.

Site No.	Location (Latitude Longitude)	Seafloor Depth (mbrf)	Operations Description	Transit (days)	Drilling Coring (days)	Logging (days)
Amsterdam			Begin Expedition 5.0 port call days			
			Transit ~1235 nmi to ALM-03B @ 10.5	4.9		
ALM-03B	37.377110° N	1638	Hole A - APC/HLAPC/XCB to refusal (~750 mbsf) - 4 ea APCT3 measurements	0	4.9	0.0
EPSP	9.598530° W		Hole B - Drill ahead to 700 mbsf - SET Temp merasurement - RCB Core to 930 mbsf -	0	3.8	1.3
to 930 mbsf			Log w/Triple Combo, FMS Sonic & VSP			
			Sub-Total Days On-Site: 10.0			
			Transit ~126 nmi to GUB-02A @ 10.5	0.5		
GUB-02A	36.699683° N	558	Hole A - APC/HLAPC/XCB to 550 mbsf - 4 ea APCT3 measurements	0	2.7	0.0
EPSP	7.431423° W		Hole B - Install Reentry system & 10-3/4" to 525 mbsf w/ HRT - SET Temp	0	8.8	1.8
to 1464 mbsf			measurement - RCB to 1464 mbsf - Log w/Triple Combo, FMS-Sonic & VSP			
			Sub-Total Days On-Site: 13.2			
			Transit ~157 nmi to WAB-03A @ 10.5	0.6		
WAB-03A	36.312544° N	811	Hole A - APC/HLAPC/XCB to 660 mbsf - 4 ea APCT3 measurements	0	3.6	0.0
EPSP	4.571213° W		Hole B - Install Reentry system & 10-3/4" w/ HRT to 650 mbsf - SET Temp	0	10.6	2.1
to 1700 mbsf			Measurement - RCB to 1700 mbsf - Log w/Triple Combo, FMS-Sonic & VSP			
			Sub-Total Days On-Site: 16.4			
			Transit ~944 nmi to Napoli @ 10.5	3.7		
Napoli			End Expedition	9.8	34.4	5.2

Port Call:	5.0	Total Operating Days:	49.4
Sub-Total On-Site:	39.6	Total Expedition:	54.4

(Blanc, 2006; Ryan and Hsü, 1973) in the latest Miocene. This event is known as the Messinian Salinity Crisis (MSC; Hsü et al., 1973). Ongoing tectonic convergence coupled with isostatic rebound related to lithospheric mantle dynamics (Duggen et al., 2003) not only severed these earlier marine connections but also uplifted and exposed them on land (Capella et al., 2017). In the early Pliocene (Table **T3**), two-way exchange was established through a single conduit, the Gibraltar Strait.

During the MSC, the amplified net evaporative flux changed to such an extent that the salinity of water flowing into the Atlantic varied between near-equality with Atlantic water (~36 g/kg) to halite-depositing brine (>360 g/kg) and brackish water conditions (<20 g/kg). Gibraltar exchange today exhibits one of the largest density contrasts in the modern ocean (Table **T1**), but this contrast was increased by up to two orders of magnitude during the acme of the MSC. The water flowing into the Atlantic at this time was probably the most extremely dense overflow of oceanographic scale in Earth's history, and all other aspects of the exchange would have been proportionally exaggerated.

The scientific aim of IMMAGE is to determine when MO first occurred and to constrain quantitatively how the Atlantic Ocean and global climate were altered as a consequence of both the inception of Atlantic–Mediterranean exchange and extreme density contrast between the two. This can only be achieved by recovering the following:

- The early record of the gateway, which is preserved onshore in Morocco and Spain (ICDP drilling);
- The later gateway record, which is preserved offshore in the Alborán Basin (IODP drilling); and
- Atlantic sediments impacted by MO (IODP drilling).

IMMAGE therefore requires an amphibious drilling strategy and is the first Land-2-Sea project. Expedition 401 is the first of the three drilling phases required to implement IMMAGE. Onshore drilling in Spain and Morocco is not yet scheduled, but is likely to be undertaken in that order.

Table T3. Operations plan and time estimates for primary sites, Expedition 401, Option 2 (see text).

Site No.	Location (Latitude Longitude)	Seafloor Depth (mbrf)	Operations Description	Transit (days)	Drilling Coring (days)	Logging (days)
Amsterdam			Begin Expedition 5.0	port call days		
			Transit ~1235 nmi to ALM-03B @ 10.5	4.9		
ALM-03B	37.377110° N	1638	Hole A - APC/HLAPC/XCB to 750 mbsf - 4 ea APCT3 measurements	0	4.9	0.0
EPSP	9.598530° W		Hole B - Drill ahead to 700 mbsf - SET Temp merasurement - RCB Core to 930 mbsf -	0	3.8	1.3
to 930 mbsf			Log w/Triple Combo, FMS Sonic & VSP			
			Sub-Total Days On-Site: 10.0			
			Transit ~126 nmi to GUB-02A @ 10.5	0.5		
GUB-02A	36.699683° N	558	Hole A - Install Reentry system & 10-3/4" to 525 mbsf w/ HRT - RCB to 1464 mbsf - Log	0	8.8	1.8
EPSP	7.431423° W		w/Triple Combo, FMS-Sonic & VSP			
to 1464 mbsf						
			Sub-Total Days On-Site: 10.6			
			Transit ~157 nmi to WAB-03A @ 10.5	0.6		
WAB-03A	36.312544° N	811	Hole A - Install Reentry system & 10-3/4" w/ HRT to 650 mbsf - SET Temp	0	10.6	2.1
EPSP	4.571213° W		Measurement - RCB to 1700 mbsf - Log w/Triple Combo, FMS-Sonic & VSP			
to 1700 mbsf			Hole B - APC/HLAPC/XCB to 660 mbsf - 4 ea APCT3 measurements	0	3.6	0.0
			Sub-Total Days On-Site: 16.4			
			Transit ~944 nmi to Napoli @ 10.5	3.7		
Napoli			End Expedition	9.8	31.7	5.2

Port Call:	5.0	Total Operating Days:	46.7
Sub-Total On-Site:	36.9	Total Expedition:	51.7

2.2. Late Miocene Climate

The mid-Cenozoic cooling trend documented by the global $\delta^{18}O_{benthic}$ record (Figure **F3A**) (Zachos et al., 2001, 2008) has been linked to the onset and growth of the East Antarctic Ice Sheet (Gulick et al., 2017). By the Late Miocene, this was well established with evidence of ephemeral continental ice sheets elsewhere (Larsen et al., 1994; St John and Krissek, 2002; Mercer and Sutter, 1982; Williams et al., 2010). Intriguingly, while deep sea cooling appears to stabilize in the Late Miocene, sea surface temperatures (SSTs) indicate up to 6°C of cooling between 7 and 5.3 Ma (Figure **F3B**) (Herbert et al., 2016). This cooling trend occurs in both hemispheres and across all of Earth's major oceans. It amplifies towards the high latitudes and terminates at 5.3 Ma, coincident with the Miocene/Pliocene boundary and the end of the MSC, with temperatures almost equivalent to modern values (Herbert et al., 2016).

This Late Miocene sea surface cooling resulted in stronger equator-pole temperature gradients, intensifying subtropical aridity and contributing to major continental ecosystem change (Herbert et al., 2016), including the expansion of C_4 plants (e.g., Dupont et al., 2013; Cerling et al., 1997). Herbert et al. (2016) attributed the cooling to a decline in Late Miocene atmospheric CO_2. Although the P_{CO2} reconstruction from this period appears to show no significant change during the Late Miocene (Foster et al., 2017), benthic carbon isotope records support a major perturbation of the global carbon cycle (Hodell and Venz-Curtis, 2006). Possible drivers of this CO_2 drawdown are sequestration in the deep ocean of eroded organic soil matter released from a less vegetated land surface (Diester-Haas et al., 2006) and ocean gateway change causing shoaling of the thermocline (LaRiviere et al., 2012). What has not previously been considered is the role of

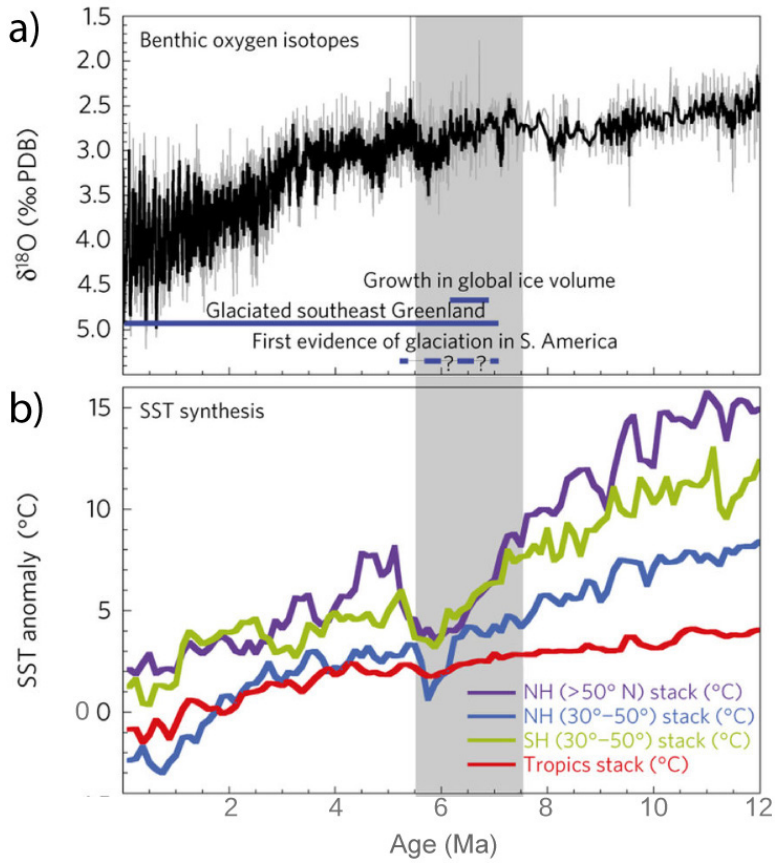

Figure F3. Seawater temperature records for (A) deep water derived from benthic $\delta^{18}O$ composite (Zachos et al., 2001) and (B) alkenone-derived SSTs for Northern Hemisphere (NH) high and midlatitudes, Southern Hemisphere (SH) midlatitudes, and Tropics (Herbert et al., 2016). Gray bar indicates the duration of the discrepancy between the implicit temperature evolution of oceanic bottom and surface water. This period ends at the Miocene/Pliocene boundary, coincident with the end of the MSC (Capella et al., 2019).

MO in oceanic circulation, the ephemeral northern hemisphere Messinian ice ages (van der Laan et al., 2012), and marine CO_2 storage during the Late Miocene (Capella et al., 2019). By recovering a record of the inception of Atlantic–Mediterranean exchange, IMMAGE drilling will be able to quantify the impact of this new source of advecting water on the Late Miocene North Atlantic, northern hemisphere glaciation, and ocean CO_2 and the other CO_2 reservoirs with which it exchanges.

2.3. Testing the global versus regional significance of the Messinian Salinity Crisis

This potential driver for global climatic change also has important implications for our understanding of the evolution of the MSC, which languishes in the grip of an enduring controversy over the relative importance of eustatic sea level change and local tectonics. Astronomical tuning of Late Miocene Mediterranean successions quashed initial hypotheses supporting the global-scale importance of the MSC (see Stanley, 1975, for a review) and suggested that regional tectonics rather than global eustatic change controlled the onset (Krijgsman et al., 1999) and termination (van der Laan et al., 2006) of the MSC. This conclusion renders the Mediterranean salt giant an extraordinary but fundamentally parochial phenomenon. Over the past few years, however, the potential global interconnectedness and significance of the MSC has revived as a result of retuning key sections (Manzi et al., 2013), a greater appreciation of the uncertainties in subprecessional phasing of Mediterranean successions (Modestou et al., 2017), the intricate history of the MSC (Hilgen et al., 2007). The generation of Late Miocene orbital resolution stable isotope records in the open ocean (e.g., van der Laan et al., 2012; Drury et al., 2017) improved understanding of the ocean-dynamic consequences of decreased global salinity arising from sinking 6% of global NaCl into the salt giant itself (Cullum et al., 2016), as well as the new SST synthesis (Herbert et al., 2016). Despite this expanding evidence base, this global versus local paradox has not been tested because we lack the high-resolution records of Atlantic–Mediterranean exchange. The precessional-scale correlation of Mediterranean and Atlantic successions will allow the IMMAGE team to test rigorously hypotheses that relate the MSC to global climatic change.

2.4. Seismic studies/site survey data

The supporting site survey data for Expedition 401 are archived at the IODP Site Survey Data Bank (**https://ssdb.iodp.org/SSDBquery/SSDBquery.php**; select P895 for proposal number).

3. Scientific objectives

The target of the IMMAGE drilling proposal is the record of Atlantic–Mediterranean exchange during the most dynamic and variable period of its history, from inception through salt giant formation to the establishment of an exchange configuration similar to today. The sediments on either side of the gateway region, which are preserved both onshore and offshore, record the changing nature of Atlantic–Mediterranean exchange, allowing quantitative evaluation of its role in global-scale climate systems, impact on major climatic events, and influence over extreme environmental change in the Mediterranean. Two of IMMAGE's scientific objectives are therefore paleoclimatic. In addition, a Late Miocene drilling target focused on the gateway also provides an unparalleled opportunity to test physical oceanographic representations of extreme high-density overflow dynamics that do not exist in the world today on this scale.

3.1. Objective 1: to document the time at which the Atlantic first started to receive a distinct overflow from the Mediterranean and to evaluate quantitatively its role in Late Miocene global climate and regional environmental change

Today, dense water (13°C, 37g/kg; Price et al., 1993) pools on the floor of the Mediterranean behind a shallow (300 m), narrow (15 km) sill, the Gibraltar Strait. Mediterranean waters overspill the sill and cascade down the continental slope. The density contrast between Mediterranean and

ambient Atlantic water generates substantial current speed, leading to extensive contouritic drifts (Hernández-Molina et al., 2016). Recent fieldwork in Morocco has revealed that the Rifian Corridor in northern Morocco contains Upper Miocene contouritic sediments (Capella et al., 2017) that resemble the Pliocene–Pleistocene contourites in the Gulf of Cadiz (IODP Expedition 339; Expedition 339 Scientists, 2013).

The presence of 7.8–6.3 Ma contourites in Morocco (Capella et al., 2017) indicates that an overspill geometry had already formed in the Late Miocene, ~2 My before the MSC, allowing a density contrast between the Mediterranean and Atlantic to develop and feeding saline Mediterranean water into the North Atlantic (Capella et al., 2017, 2019). The outstanding question is whether these exposed Rifian contourites are the first products of MO or whether older, buried contourites exist in either the Rifian and/or Betic corridors (Figures **F2**, **F4**).

One possibility is that initiation of MO contributes to the cooling that ultimately triggers the formation of permanent Northern Hemisphere ice by altering the North Atlantic density structure and increasing CO_2 drawdown through the entrainment of Atlantic surface water and its dissolved CO_2 in the dense AMW plume (Capella et al., 2019). Correlation with similarly high-resolution sites in the North Atlantic will be required to test this mechanism and assess its importance in modulating NADW formation. Correlation with Messinian sequences recovered during IODP Expeditions 346 (Japan Sea) and 361 (Agulhas Current) will allow us to evaluate the influence of the MSC on atmospheric conditions and continental-scale aridification (Zhang et al., 2014).

Hypotheses that will be tested as part of this scientific objective include the following:

- Hypothesis 1.1: the earliest contourites formed as a result of Atlantic–Mediterranean exchange, correlate with the onset of Late Miocene SST decline in the mid- and high latitudes. Dating the first Atlantic–Mediterranean contourites will test this hypothesis.
- Hypothesis 1.2: atmospheric CO_2 sequestration in the deeper ocean through the initiation and development of AMW can account for the degree and distribution of SST cooling observed. Reconstructing the velocity, density, and flux of AMW through time, quantifying its impact on CO_2 advection (Capella et al., 2019), and then modeling the resulting SST distribution (e.g., Ivanovic et al., 2014a) tests this hypothesis.

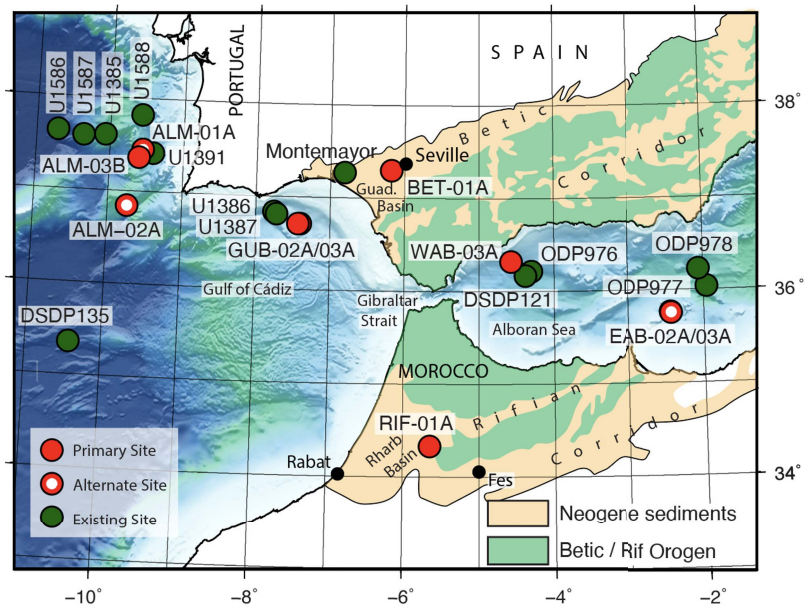

Figure F4. Map of the Mediterranean–Atlantic gateway at Gibraltar and the two Miocene connections, the Betic and Rifian corridors, that are now exposed on land in Spain and Morocco respectively. Red circles indicate IMMAGE IODP Expedition 401 and ICDP primary drilling targets; red circles with white centers indicate alternate sites. Green dots indicate existing IODP/ODP/DSDP sites and the Montemayor borehole, which recovered Upper Miocene sediments. Sites closest to Expedition 401 sites that did not reach the Miocene (U1385, U1588, and U1391) are also plotted in green.

- Hypothesis 1.3: Atlantic–Mediterranean Water modulates NADW formation, triggers glacial inception, and influences continental-scale aridification. Model-based testing of this hypothesis requires the correlation of IMMAGE records with existing high-resolution records globally.

3.2. Objective 2: to recover a complete record of Atlantic–Mediterranean exchange before, during, and after the Messinian Salinity Crisis and to evaluate the causes and consequences of this extreme oceanographic event locally, regionally and globally

Today, Mediterranean seawater flows through the Gibraltar Strait forming a saline plume at intermediate depths in the Atlantic (Iorga and Lozier, 1999). The plume's record of Pliocene–Quaternary contouritic sediments was recovered from the Gulf of Cadiz (IODP Expedition 339) and documents a Mediterranean contribution to Atlantic thermohaline circulation since the Pliocene (Hernández-Molina et al., 2014b; van der Schee et al., 2016; Garcia-Gallardo et al., 2017a, 2017b). However, there was also a Late Miocene episode of Mediterranean influence on the Atlantic (Capella et al., 2017, 2019) although the conduit for Atlantic–Mediterranean exchange is unclear because Gibraltar may have already been open alongside marine corridors in northern Morocco and southern Spain (Figure **F4**) (Flecker et al., 2015; Martín et al., 2009; Krijgsman et al., 2018) and the Alborán Basin may have been an intermediate system separated from the Mediterranean by the Alborán volcanic arc (Booth-Rea et al., 2018). The sedimentary expression of restriction and closure of these Miocene connections in the Mediterranean comprises both thick evaporites (e.g., Roveri et al., 2014) and brackish "Lago Mare" sediments (Figure **F5**) (Iaccarino and Bossio, 1999; Orszag-Sperber, 2006; Rouchy et al., 2007; Guerra-Merchan et al., 2010). Understanding the causes of high-amplitude salinity change in the Mediterranean and its global consequences depends on recovering a complete record of Atlantic–Mediterranean exchange before, during, and after the MSC.

Hypotheses that will be tested as part of this scientific objective include the following:

- Hypothesis 2.1: the Alborán Basin was an intermediate marine system influenced by the Atlantic and separated from the Mediterranean by the Alborán volcanic arc during the MSC.
- Hypothesis 2.2: extreme environmental fluctuations in the Mediterranean had negligible impact on AMW.

Both hypotheses require the reconstruction and comparison of physical properties of Late Miocene water in the Atlantic (proposed Site ALM-01A), Alborán Sea (proposed Site WAB-03A), and existing Mediterranean successions.

3.3. Objective 3: to test our quantitative understanding of the behavior of ocean overflow plumes during the most extreme exchange in Earth's history

There are ~20 major ocean-scale overflow systems in the world today (Legg et al., 2009), including some of the most important and sensitive oceanic transport systems (e.g., Denmark Strait and Weddell Sea). All of these systems are driven by source water density anomalies upstream of the overflow (Price and O'Neill-Baringer, 1994). However, the range of source water density today is rather small; 27.7 s units (Red Sea) to 28.95 s units (Mediterranean Sea) (Table **T1**). In comparison, the density of Mediterranean water during gypsum (Stages 1 and 3 of the MSC) (Figure **F5**) and halite deposition (Stage 2) would have been enormous (110 and ~300 s units respectively). This presents an opportunity and a challenge for existing representations of oceanographic overflow physics (e.g., Legg et al., 2009) because we can test hypotheses derived from physical theory through scientific drilling. This is the first experiment of its type that we are aware of and is ground-breaking in the field of quantitative paleoceanography.

The application of physical theory to the paleoceanography of MO is well established (Rogerson et al., 2012a) and suggests the following hypotheses:

- Hypothesis 3.1: the velocity of the plume is a function of the Atlantic–Mediterranean density contrast, limitation on flow through the strait (Bryden et al., 1994), the gradient of the slope, and the degree of mixing (Price et al., 1993).
- Hypothesis 3.2: mixing with ambient water causes a strong negative feedback on the size of the plume, limiting the degree of its variability (Price et al., 1993). This means that only minor changes in the physical size of the plume are expected, despite the proportion of plume water derived directly from the outflow varying significantly. As a result, changes in Mediterranean density have little impact on the plume position.
- Hypothesis 3.3: the main control on the settling depth of MO is the vertical density gradient in the North Atlantic, which is a product of North Atlantic overturning circulation (Rogerson et al., 2012a).

These qualitative hypotheses have been quantitatively investigated in pilot experiments exploring a range of MSC-like salinity scenarios. They show that only minor changes in the position and size of the MO plume result from extreme differences between evaporite depositing (MSC) and Lago Mare (brackish-water) boundary conditions (Figure **F6**). The brackish plume lies at the depth of the upper part of the modern MO (Borenäs et al., 2002), whereas the evaporite plume coincides with the lower part of the modern flow. In phases, the plume extends over roughly half the area influenced by the modern plume. The response of MO settling depth to the North Atlantic density gradient is shown in Figure **F6D**. As Miocene AMOC may have been either lower or higher than today (Butzin et al., 2011; Panitz et al., 2018), the position of the plume could be either higher or

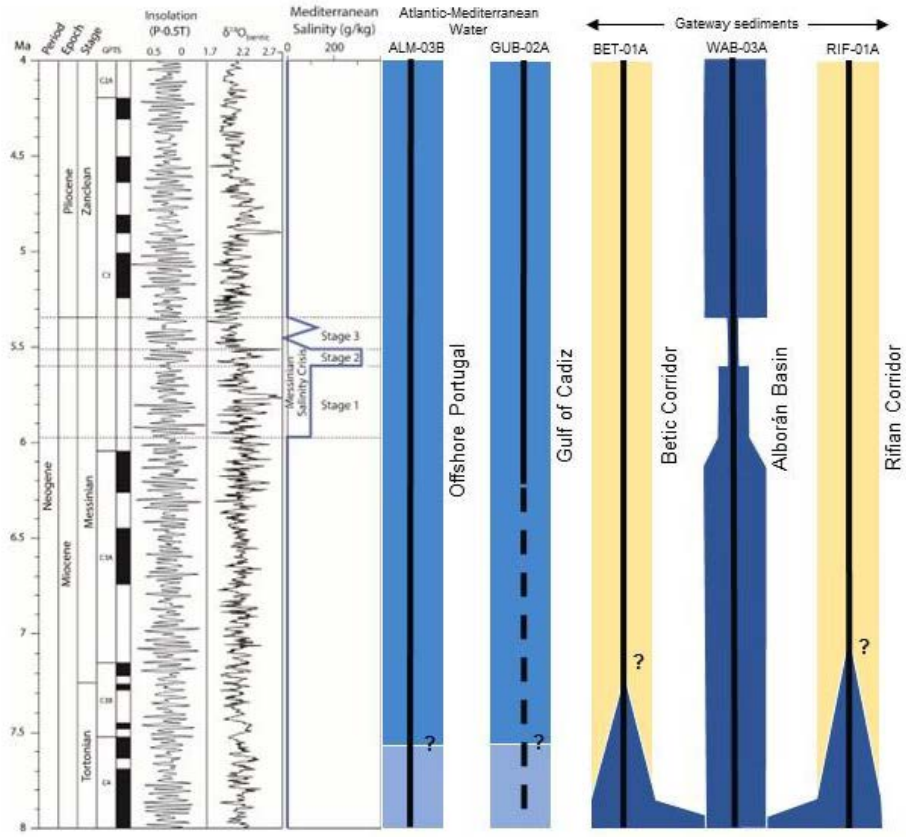

Figure F5. Temporal range of IMMAGE sites. Dark blue indicates higher density Mediterranean water, with the width of the Alborán Basin column indicative of the gateway restriction. Intermediate blue represents AMW, and pale blue indicates the Atlantic water prior to the onset of MO. Yellow indicates continental sediments that accumulated in the Betic and Rifian corridors once marine exchange through them had terminated. A reconstructed salinity profile of Mediterranean water through time (Flecker et al., 2015) illustrates the enhanced salinity during the three stages of the MSC. Insolation (Lourens et al., 1996), which has a strong precessional component that is reflected in the sedimentary record, the benthic foraminifera $\delta^{18}O$ curve generated for the Salé Core, Morocco (Hodell et al., 2001), and the Pliocene–Pleistocene stack (Lisiecki and Raymo, 2005) are plotted alongside.

lower on the slope than indicated in Figure **F6A–F6C** and will also vary on orbital timescales because this forcing is expected to cause variations in AMOC (Panitz et al., 2018), but to a much smaller extent than during the Pleistocene.

These results suggest that both secular and cyclic changes in the position of the plume will be recorded in its sedimentary product and that the position of the plume is almost independent of Mediterranean salinity. Coring locations based on the modern plume position, Late Miocene paleogeography of the coastline and slope, and seismic evidence of Late Miocene contouritic sedimentation should recover the full Late Miocene record of exchange. Site GUB-02A will target plume sediments immediately downstream of the gateway (Figure **F4**), and Site ALM-02A will provide a record of the plume at equilibrium depth. The targeted sites will provide high-resolution records that complement, but do not replicate Expedition 397 Sites U1586 and U1587, which are more distal.

The opportunity to integrate physical and geological oceanography envisaged here is unique and exciting, and it ensures that regardless of the record we recover, the results will have far-reaching implications. IMMAGE is a direct hypothesis test, investigating whether the representations of overflows within general circulation models are effective outside the range of validation provided by the modern ocean. If the record fulfills the predicted patterns (Figure **F6**), this will, for the first time, provide empirical evidence that these representations are adequate under extreme boundary conditions. Moreover, this success would allow us to embed physical oceanography more explicitly in our interpretation of the record, laying the foundation for a new and fully quantitative understanding of the past. If the record is inconsistent with the hypotheses, this will be an important, empirical challenge to assumptions used in climate modeling, casting doubt on all modeling experiments in which part of the ocean-atmosphere system is outside the range exhibited today. We are not aware of a previous case where scientific drilling has been used to test ocean physics hypotheses as explicitly as we propose here. Extreme differences between our predictions and core evidence which are nevertheless resolvable by iterative modeling, for example an extremely deep plume comparable to late Quaternary Heinrich Events (Rogerson et al., 2012a), will also be incom-

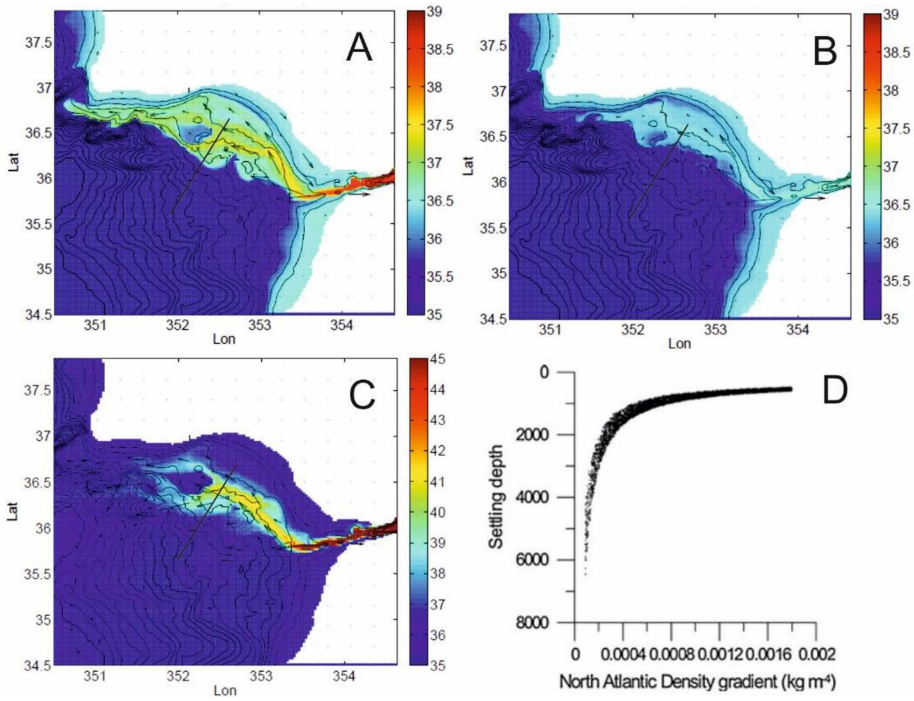

Figure F6. Salinity (color) and velocity field (arrows) for simulated MO at different time periods, showing the size and location of the resulting overflow plume in the Gulf of Cadiz. A. Modern configuration. B. Lago Mare (brackish water) submaximal exchange. C. MSC gypsum depositional phases. D. Impact of altering Atlantic vertical density gradient on the setting depth of MO Water (Rogerson et al., 2012a).

patible with current conceptualization of how the Miocene Atlantic operated and will provide very high-impact results.

4. Connections to the 2050 Science Framework

Expedition 401 and IMMAGE drilling are relevant to the following parts of the 2050 Framework for scientific ocean drilling.

4.1. Strategic objectives

4.1.1. Earth's climate system

Opening and closure of oceanic gateways is recognized as having a profound impact on Earth's climate, changing the distribution of heat and salt in the world's oceans. Dense salty water from the Mediterranean contributes to thermohaline circulation, NADW formation, and associated carbon drawdown.

4.1.2. Tipping points in Earth's history

Flooding of the Mediterranean basin at the end of the Miocene is one of the most vivid examples of a tipping point in Earth's history. However, the history of water flow through this gateway remains to be described in detail, and it has consequences not just for the Mediterranean but also for the global ocean.

4.1.3. Global cycles of energy and matter

The Mediterranean-Atlantic Gateway has a controlling influence on the distribution of salt, heat, and nutrients in the ocean.

4.2. Flagship initiatives

4.2.1. Groundtruthing future climate change

Sediment cores from this expedition will cover the last ~8 Ma of Earth's climate, including analogs for future warm climates under CO_2 levels up to ~500 ppm. In particular, the combination of gateway and climate history recorded in the cores will help us understand global climate from 5 to 8 Ma, a relatively understudied interval compared to the last 5 My.

4.3. Enabling elements

4.3.1. *Broader impacts and outreach*

We aim to reach a broad audience to communicate the expedition's science and real-time progress. Because of the unusually long duration of this Land-2-Sea drilling project, we have an opportunity to develop a more ambitious outreach endeavor than is typical and will be targeting, in particular, communities that do not normally engage with scientific narratives. This will include a cocreation project called Earth System Song and a multisensory exhibition known as the Mobile Science Sensorium.

4.3.2. *Land to sea*

This IODP expedition is the first element of the first ever Land-2-Sea drilling project. The onshore ICDP drilling will happen in the years following Expedition 401 at sites in southern Spain and northern Morocco. Integrated results from both the land and sea drilling are necessary to fully understand Late Miocene gateway history and deliver IMMAGE's scientific objectives.

5. Operations plan

5.1. Coring strategy

The expedition will drill at three primary sites. At Site ALM-03B, west of Portugal, we aim to recover a thick Late Miocene succession of distal MO deposits. Site GUB-02A, in the Gulf of

Cadiz, targets a high-resolution (precessional) record of Late Miocene MO at an intermediate site between the proposed onshore ICDP sites (RIF-01A and BET-01A) and the distal Site ALM-03B. Site WAB-03A targets one of the few thick late Messinian sedimentary successions in the Alborán basin to provide key constraints on the chemistry and physical properties of MO water during and after the MSC.

Critical to the success of the science is the ability to correlate each site at a precessional scale, both with each other, with the onshore IMMAGE sites, and with global climate and paleoceanographic records. Ideally, this would be achieved through recovering a complete core record of Atlantic–Mediterranean exchange during the Late Miocene–early Pliocene. However, there are only a few sites where the Late Miocene offshore is sufficiently shallow to be accessible to drilling with *JOIDES Resolution*. This means that the intervals we are targeting are typically quite deeply buried at depths where core recovery is likely to be <100%. They are buried at similar depths at the onshore sites too, but because we will use mining drilling technology (not possible to deploy on a moving ship), we can expect a core recovery much closer to 100%. To meet the requirement of precession-scale correlation, the IMMAGE drilling strategy will use both stratigraphic information derived from recovered cores and high-resolution logging data (i.e., Formation Image logs supplemented with standard gamma ray, photoelectric effect [PEF], neutron porosity, density, resistivity, and sonic logs), from which we anticipate a much higher likelihood of recovering a full stratigraphy.

All of the targeted sediments are anticipated to record a precessional pulse derived from the African monsoon and North Atlantic storm tracks (Marzocchi, 2016) that is visible in both the chemical and physical components of the core and in the logging data. These successions also show characteristic eccentricity modulation that will provide astrochronological tie points in addition to bio- and magnetostratigraphic age constraints. The use of industrial logging data for astronomical tuning was demonstrated in the Guadalquivir Basin close to Site BET-01A (Ledesma, 2000). Our strategy is to construct a precessional framework at each site using the high-resolution logging data combined with stratigraphic information provided by the recovered cores. For more information on the downhole logging tools, see **http://iodp.tamu.edu/tools/logging**.

At the time of writing, we are submitting a request to the EPSP to extend drilling at Site GUB-02A from the current maximum permitted depth of 930 metes below seafloor (mbsf), part-way through the Messinian, to 1464 mbsf, in the Tortonian. Permission depends on the anticipated absence of hydrocarbon hazards at this location. The time estimates in this prospectus assume drilling to 1464 mbsf; if we do not receive permission for this depth, then operational time will become available either as contingency for lost time (due to weather or drilling problems) or for additional coring.

The three Expedition 401 sites are relatively deep, and the main scientific targets are in the bottom part of each hole. Time estimates for drilling, logging, and coring from the seafloor to the target depths at all three sites currently leave some contingency time, but there is still a risk that we may not reach the depth and science objectives at the final site if there is any delay in operations. For comparison, IODP Expedition 397 (Iberian Margin) lost 8 days of operations time because of high seas. However, all three sites are quite close to existing IODP/Integrated Ocean Drilling Project/ODP/DSDP sites where the Quaternary was previously recovered and is available for sampling. Usually at new drilling sites, the first hole must be cored continuously from the seafloor to make hydrocarbon safety measurements on each core. We are in the process of proposing to EPSP to build in some contingency time by applying existing gas measurements from existing sites close to Sites GUB-02A and WAB-03A and washing down through part or all of the Pleistocene section before starting to core and log from or just above the top of the Pliocene, drilling only a single hole at one or both of these sites. This approach is subject to EPSP approval for each of these two sites, and the exact drilling strategy will vary depending on water depth, total penetration target depth, and the need for casing. This drilling strategy is described as Option 2 for Sites GUB-02A and WAB-03A (Figures **F7**, **F8**). Option 1 for each site is the drilling strategy where for safety reasons we are required to monitor for hydrocarbons down all sections of the holes we drill rather than using existing data from adjacent sites. It is not unlikely that some combination of Options 1 and 2 will ultimately be implemented. We do not propose to request the option to wash down at Site

ALM-03B because the Pliocene/Pleistocene boundary is only at 85 mbsf and will therefore not save much time. The options at each of the three primary sites are described below.

5.1.1. Site ALM-03B

We will drill using the advanced piston corer (APC) and extended core barrel (XCB) systems and attempt to get to the target depth of 930 mbsf. If this is not possible because coring becomes too slow with the XCB system, an additional hole will be drilled using the rotary core barrel (RCB) system, washing down the previously recovered interval and then coring to the target depth.

5.1.2. Site GUB-02A

Option 1: if we need to generate our own gas measurements for safety reasons, the drilling strategy is as follows:

- Core Hole A with the APC and XCB systems to the depth at which the casing needs to be set (525 mbsf), taking gas measurements. This should be above the Pliocene/Pleistocene boundary. If EPSP permission to core to 1464 mbsf is not granted, we would attempt to core as deeply as possible to the current maximum permitted depth of 920 mbsf with the APC and XCB systems.
- If the target depth is 920 mbsf and was not reached in Hole A, wash Hole B down to the depth that APC/XCB coring reached and core with the RCB system to 920 mbsf.
- If the target depth is 1464 mbsf, case Hole B to 525 mbsf and core with the RCB system to 1461 mbsf.

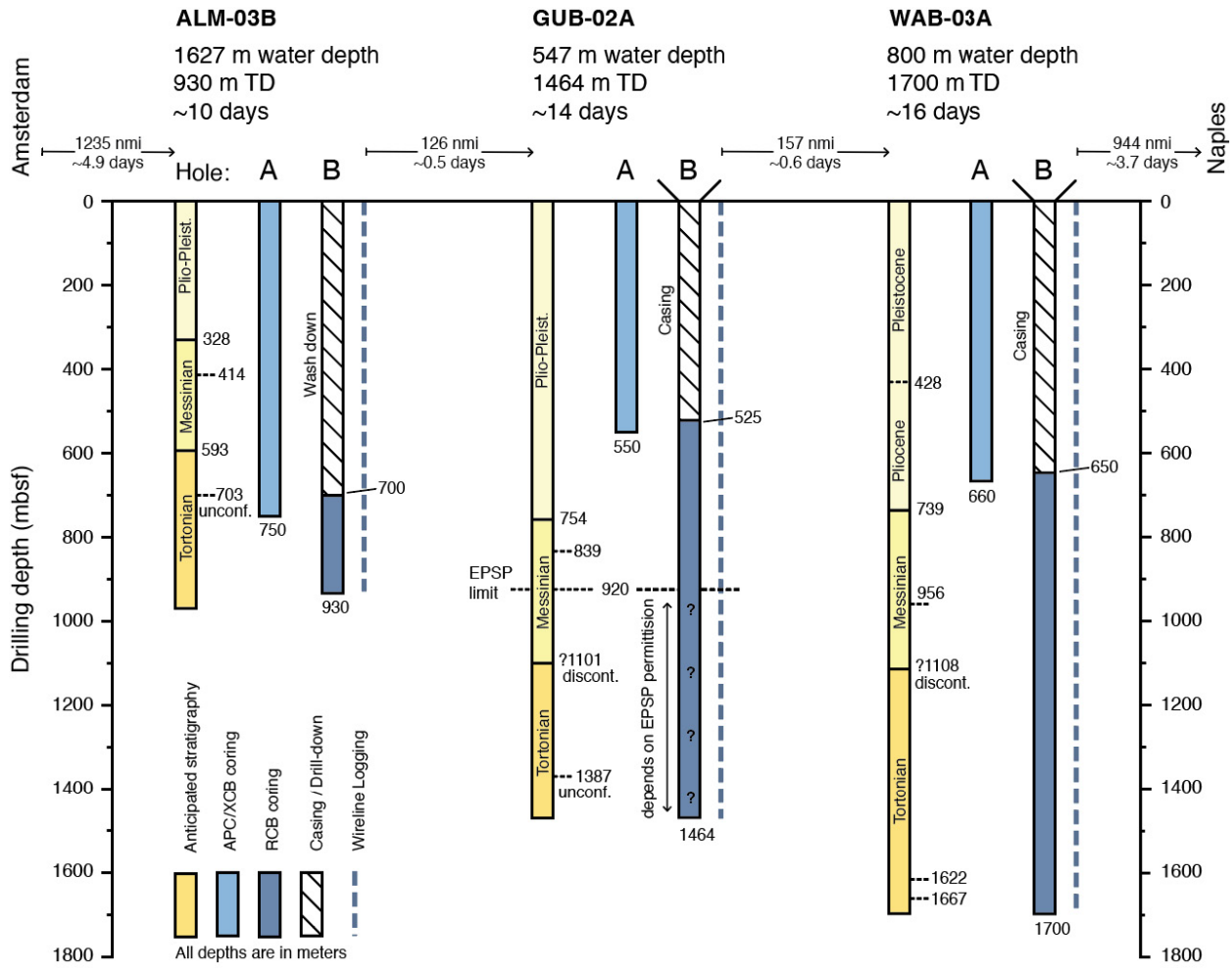

Figure F7. Option 1 drilling, coring, and logging strategy where hydrocarbon monitoring down the full length of holes drilled during Expedition 401 is required. TD = total depth.

- Complete the full logging program to the target depth (obtaining a natural gamma ray log through the casing for the top 525 m).

Option 2: if we are allowed by the EPSP to use the gas measurements from Expedition 339 Sites U1387 and U1386 (~36 km northwest) instead of generating these ourselves, the single-hole drilling strategy is as follows:

- If permission is given to core to 1464 mbsf, wash down Hole A to 525 mbsf and case this upper part of the hole. Otherwise, do not install casing.
- Core (RCB system) and log Hole A from 525 mbsf to the bottom of the hole (obtaining a natural gamma ray log through the casing for the top 525 m).

This would save ~2.5 days relative to Option 1.

5.1.3. Site WAB-03A

Option 1: if we need to generate our own gas measurements for safety reasons, the drilling strategy is as follows:

- Core Hole A with the APC and XCB systems to a depth just below where the casing needs to be set (660 mbsf), taking gas measurements.
- Case Hole B to 650 mbsf.
- Core Hole B with the RCB system to the target depth of 1700 mbsf.

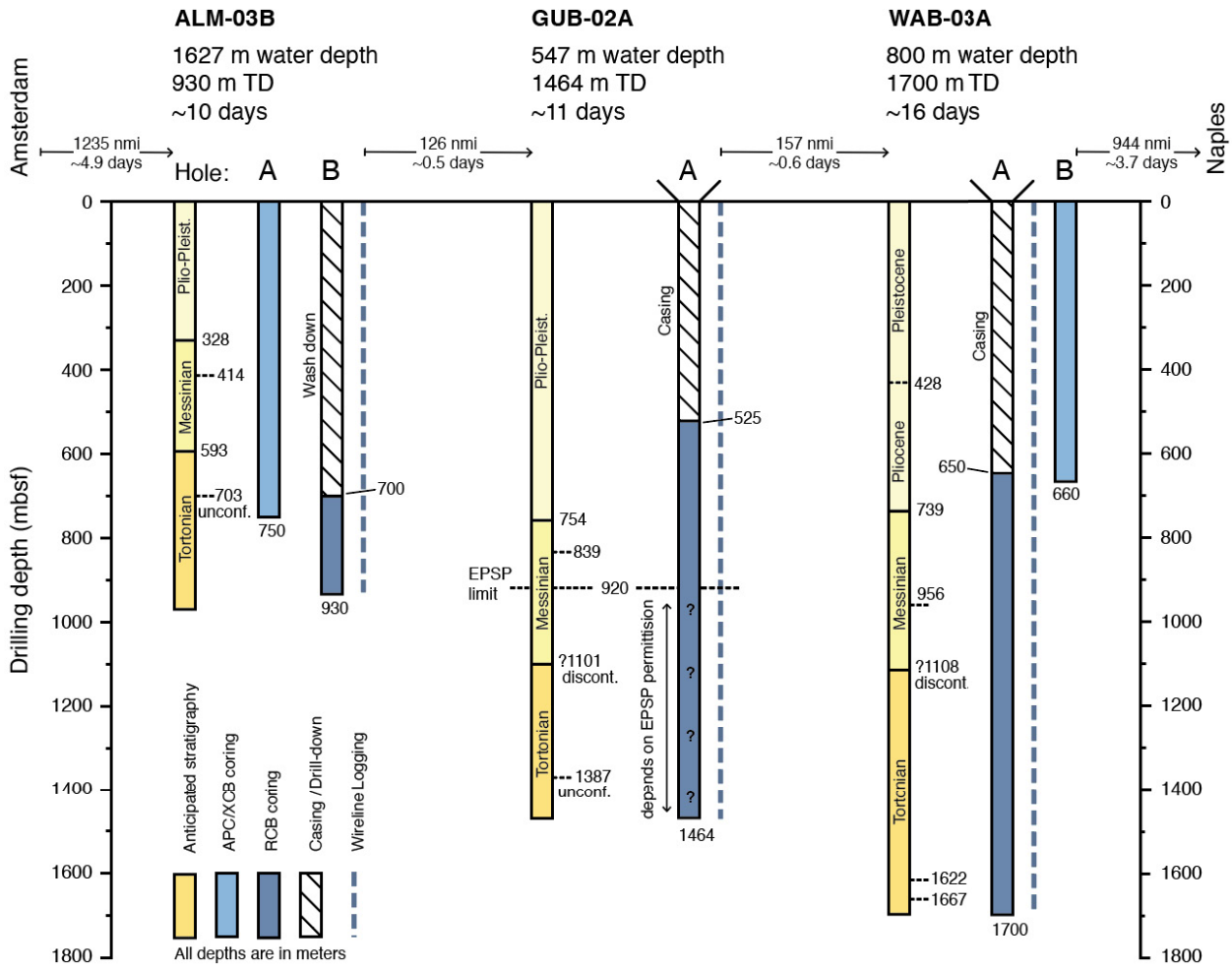

Figure F8. Option 2 drilling, coring, and logging strategy where the EPSP permits the use of hydrocarbon measurements from existing adjacent IODP/ODP/DSDP sites. TD = total depth.

- Complete the full logging and coring program from 650 mbsf to the target depth. This will also produce a natural gamma ray record through the casing for the top 650 m.

Option 2: if we are allowed to use the gas measurements from nearby DSDP Site 121 and ODP Site 976 (~25 and ~32 km away, respectively) instead of generating these ourselves, then the drilling strategy is as follows:

- Case Hole A to 650 mbsf. This is below the Pliocene/Pleistocene boundary to maximize our chances of recovering this very deep Late Miocene target interval.
- Core (RCB system) and log Hole A from 650 mbsf to the target depth of 1700 mbsf.
- Core Hole B (APC and XCB systems) to 660 mbsf with the possibility to continue coring if operational time remains.

This would not save time relative to Option 1, but it gives us more time to deal with problems should they arise if we do not leave the deepest hole until the last operation of the expedition.

If operations run according to schedule and without problems, depending on time, we may drill at one of the alternate sites:

- The Pliocene–Pleistocene at Site U1385 was recovered to ~4.5 Ma during Expedition 397, but the Miocene was not recovered. Adjacent sites indicate that Site U1385 is likely to record an excellent cyclic Late Miocene record with good carbonate preservation.
- One of the EAB sites in the eastern Alboran Basin would recover the Miocene and Pliocene.

5.2. Proposed drill sites

Sites are described from west to east, which is the proposed order of drilling during Expedition 401, apart from alternate Site U1385, which is described last.

5.2.1. Site ALM-03B (primary)

Site ALM-03B is at 1567 meters below sea level (mbsl) (Figure **F9**). The primary objective of this site is to recover a thick, shallowly buried Late Miocene succession that contains distal MO deposits. The main contribution of this site is that it will provide a record of the plume once it has reached equilibrium depth and hence help test quantitative constraints on the behavior of dense overflows (Objective 3). In addition, the high-resolution (precessional) record we will recover at this site is a key component of the complete record of Mediterranean–Atlantic exchange during the Late Miocene–Pliocene (Objectives 1 and 2). This site is close to Site U1391 (Expedition 339). The Pliocene–Quaternary (0–5.33 My) is between 0 and 258 mbsf with an average accumulation rate estimated to be ~48 m/My with hemipelagites and muddy contourites. The base of the Messinian Transparent Unit (5.6 My) is expected at 410 mbsf. This unit should be mainly hemipelagites with an average rate estimated to be ~562 m/My. Between 410 and 704 mbsf (5.6–7.2 My), Messinian contourites are expected with an average rate of ~183 m/My. The total penetration is planned to reach the Tortonian (11.9 My) at 990 mbsf. Proposed deposits of this unit are hemipelagites, contourites, and turbidites, with an average rate of ~65 m/My.

5.2.2. Site ALM-02A (alternate)

Site ALM-02A is at 2265 mbsl (Figure **F10**) and is the alternate to Site ALM-03B. It has the same main objectives. The estimate lithologies are the same, but key reflectors have deeper depths: the base of the Pliocene–Quaternary (5.33 My; 693 mbsf) has an average accumulation rate of ~130 m/My, the Messinian Transparent Unit (5.33–5.6 My; 693–874 mbsf) has an average rate of ~670 m/My, Messinian contourites (5.6–7.2 My; 874–1209 mbsf) have an average rate of ~334 m/My, and the Tortonian (7.2–11.6 My; 1209–1629 mbsf) has an average rate of ~50 m/My.

5.2.3. Site ALM-01A (alternate)

Site ALM-01A is at 1634 mbsl (Figure **F11**) and is the second alternate site to Site ALM-03B. It has the same main objectives. The estimate lithologies are also the same, and key reflectors have close depths: the base of the Pliocene–Quaternary (5.33 My; 328 mbsf) has an average accumulation rate of ~62 m/My, the Messinian Transparent Unit (5.33–6.4 My; 328–414 mbsf) has an average rate of ~80 m/My, Messinian contourites (6.4–7.2 My; 414–593 mbsf) have an average rate of

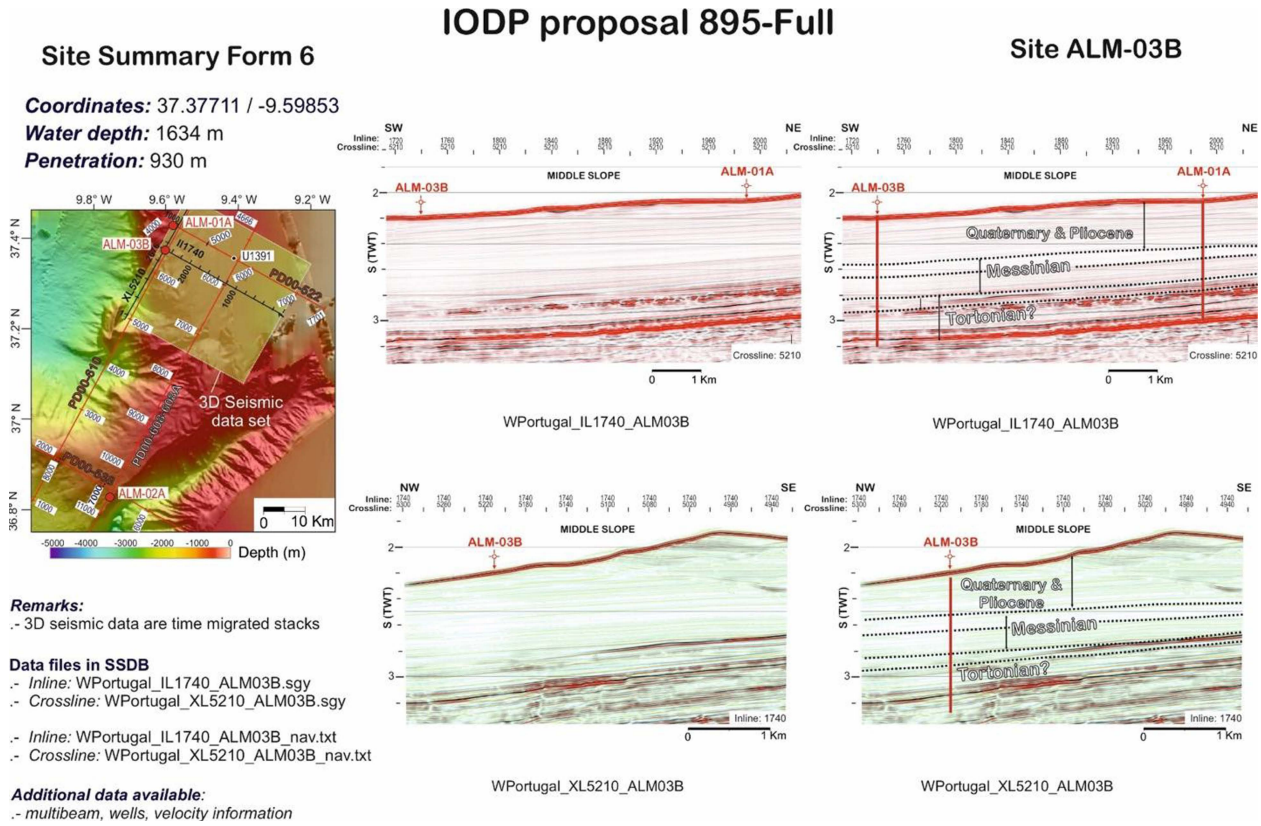

Figure F9. Site summary form for primary Site ALM-03B.

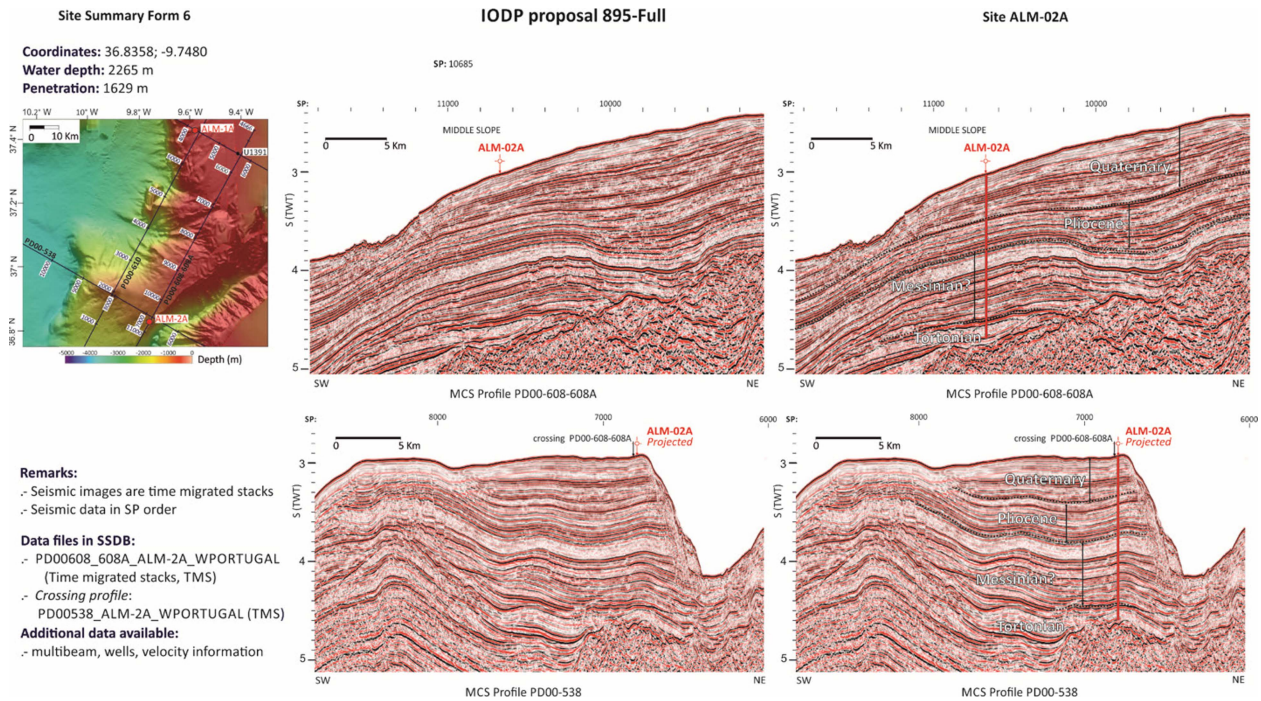

Figure F10. Site summary form for alternate Site ALM-02A.

~223 m/My. The Tortonian is divided into two units. The Upper Tortonian, down to the intra-Tortonian Unconformity (7.2-8 My; 593–703 mbsf) is estimated to have an average accumulation rate of ~138 m/My, and the Tortonian below this unconformity (8–11 My; 703–930 mbsf) has an average rate of ~75 m/My.

5.2.4. Site GUB-02A (primary)

Site GUB-02A is at 547 mbsl (Figure **F12**) and is mostly influenced by the upper branch of MO since its onset. This site targets a complete Late Miocene succession in the pathway of MO. The aim is to obtain a high-resolution (precessional) record of Miocene MO at an intermediate site between the onshore records (Sites RIF-01A and BET-01A) and the distal record (Site ALM-01A). This record makes a critical contribution to all three objectives. This site is close to Expedition 339 Sites U1386–U1389 and U1390. Average accumulation rates are estimated to be ~141 m/My to the base of the Pliocene (0–5.33 My; 0–754 mbsf), with mud and silty sand lithologies related to hemipelagites and contourites. In the Messinian Transparent Unit (5.33–6.4 My; 754–840 mbsf), average rates are ~80 m/My, associated with nannofossil marls in hemipelagites. During the Lower Messinian (6.4–7.2 My; 840–920 mbsf), sands, silty sands, and muds accumulate as hemipelagites, contourites, and turbidites, with average rates estimated to be ~327 m/My.

An application to EPSP to extend drilling at this site down to the Tortonian is currently in progress, and the drilling at this site may be revised in the light of their decision.

5.2.5. Site GUB-03A (alternate)

Site GUB-03A is at 540 mbsl (Figure **F13**). It serves as an alternate site to Site GUB-02A and thus has the same main objectives. The estimate lithologies are the same, and key reflectors have very close depths: the base of the Pliocene–Quaternary (5.33 My; 736 mbsf) has an average accumulation rate of ~138 m/My, the Messinian Transparent Unit (5.33–6.4 My; 736–869 mbsf) has an average rate of ~124 m/My, and the Lower Messinian (6.4–7.2 My; 869–930 mbsf) has an average rate of ~433 m/My.

An application to EPSP to extend the drilling at this site down to the Tortonian is currently in progress, and the drilling at this site may be revised in the light of their decision.

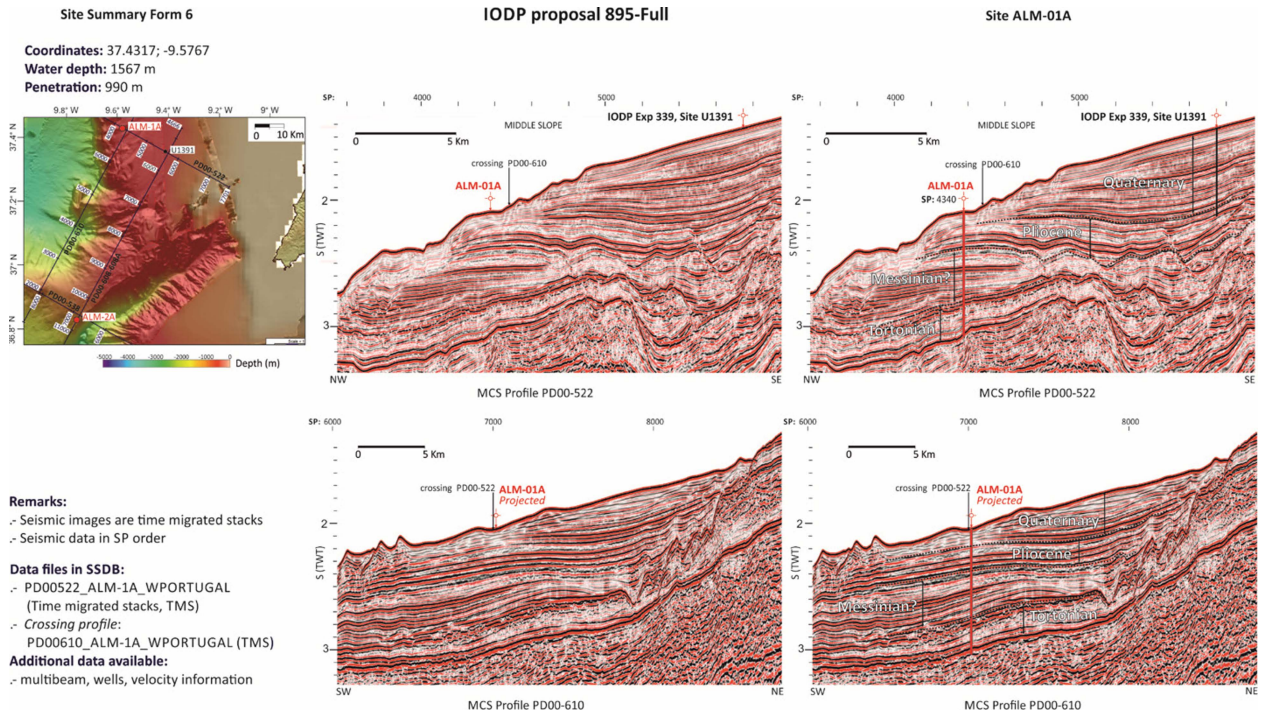

Figure F11. Site summary form for alternate Site ALM-01A.

5.2.6. Site WAB-03A (primary)

Site WAB-03A is at 800 mbsl (Figure F14). This site targets one of the few thick late Messinian sedimentary successions in the Alborán Basin. The record recovered from this location will provide key constraints on the chemistry and physical properties of MO during the Late Miocene. This is critical for all objectives. This site is close to DSDP Site 121 and ODP Site 976. The proposed total penetration is 1700 m. Quaternary (0–2.6 My; 0–428 mbsf) and Pliocene (2.6–5.33/5.46 My; 465–739 mbsf) sedimentation would be characterized by turbidites and contourites with an average accumulation rate estimated to be ~150 m/My for the two periods. The MSC (5.33/5.46–5.97 My; 739–956 mbsf) sedimentation would be subaerial/shallow waters with an average accumulation rate estimated to be ~176 m/My. The rest of the Messinian (5.97–7.2 My; 956–1108 mbsf) sedimentation would be from a deep sea environment. Tortonian, including the Tortonian tectonic inversion (7.2 to >8 My; 1108–1700 mbsf) sedimentation would be dominated by hemipelagites with average accumulation rate of ~190 m/My.

5.2.7. Site EAB-02A (alternate)

Site EAB-02A is at 845 mbsl (Figure F15). Its serves as an alternate site to Site WAB-03A and thus has the same objectives. It is located on the Spanish side of the Moroccan/Spanish territorial boundary, very close to the other alternate Site EAB-03A. This site is also close to DSDP Site 121 and ODP Sites 976–979. The Quaternary (0–2.6 My; 0–465 mbsf) and Pliocene (2.6–5.33/5.46 My; 465–715 mbsf) would be characterized by deep sea sedimentation and contourites with an average accumulation rate estimated to be ~150 m/My for the two periods. The Upper Miocene (5.33/5.46 to <7.2 My; 715–1277 mbsf) sedimentation would be open marine.

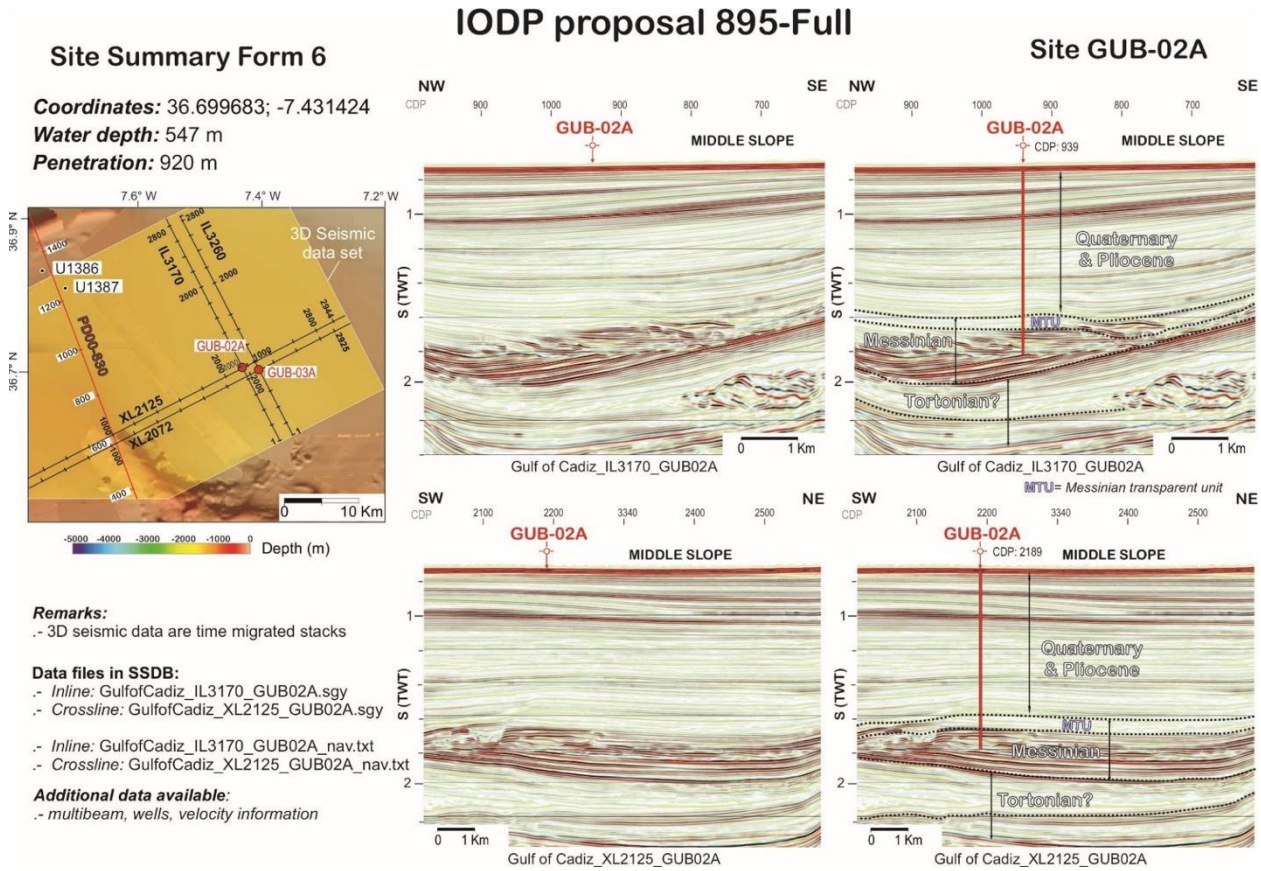

Figure F12. Site summary form for primary Site GUB-02A. These figures show the currently approved drilling depth of 920 mbsf, not the deeper penetration depth of 1464 mbsf we are currently asking EPSP to approve.

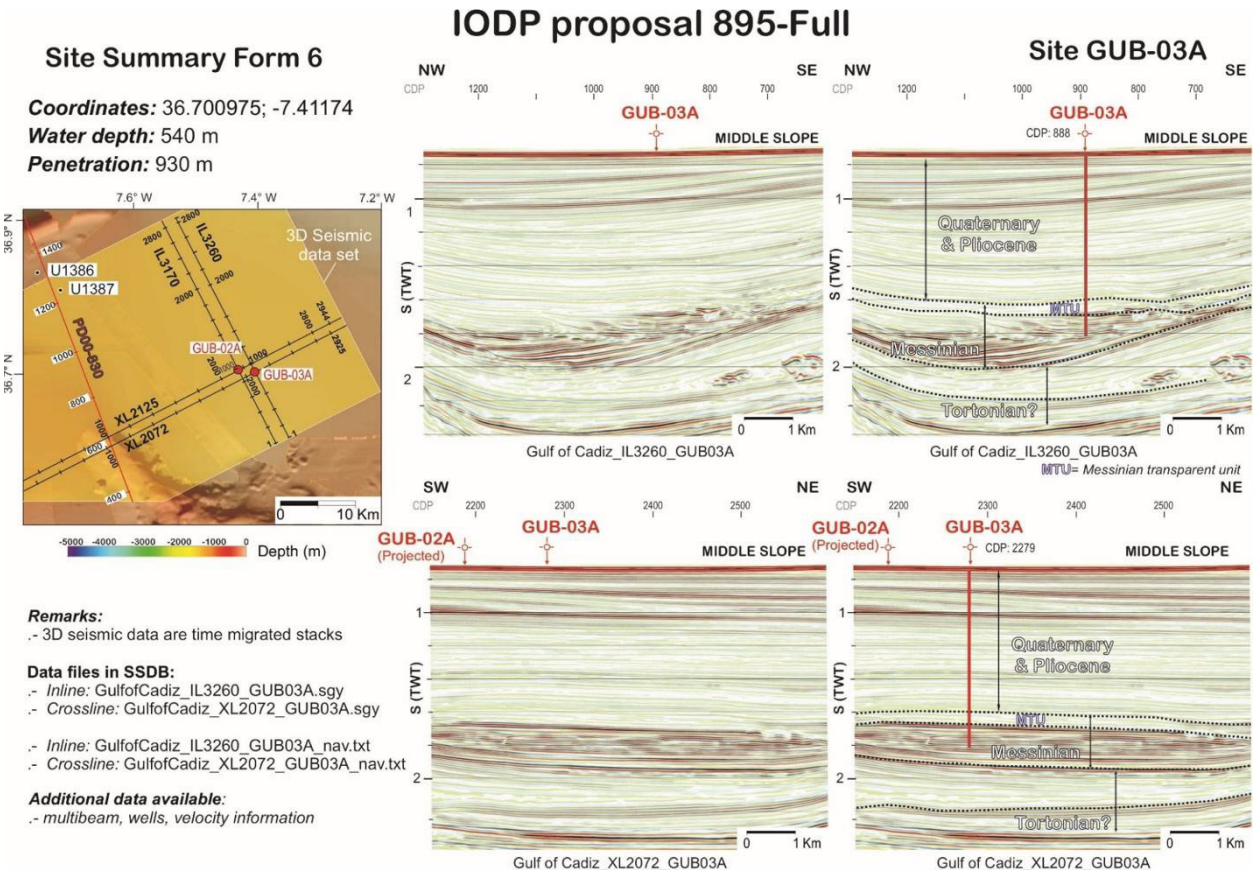

Figure F13. Site summary form for alternate Site GUB-03A. These figures show the currently approved drilling depth of 930 mbsf, not the deeper penetration depth of 1464 mbsf we are currently asking EPSP to approve.

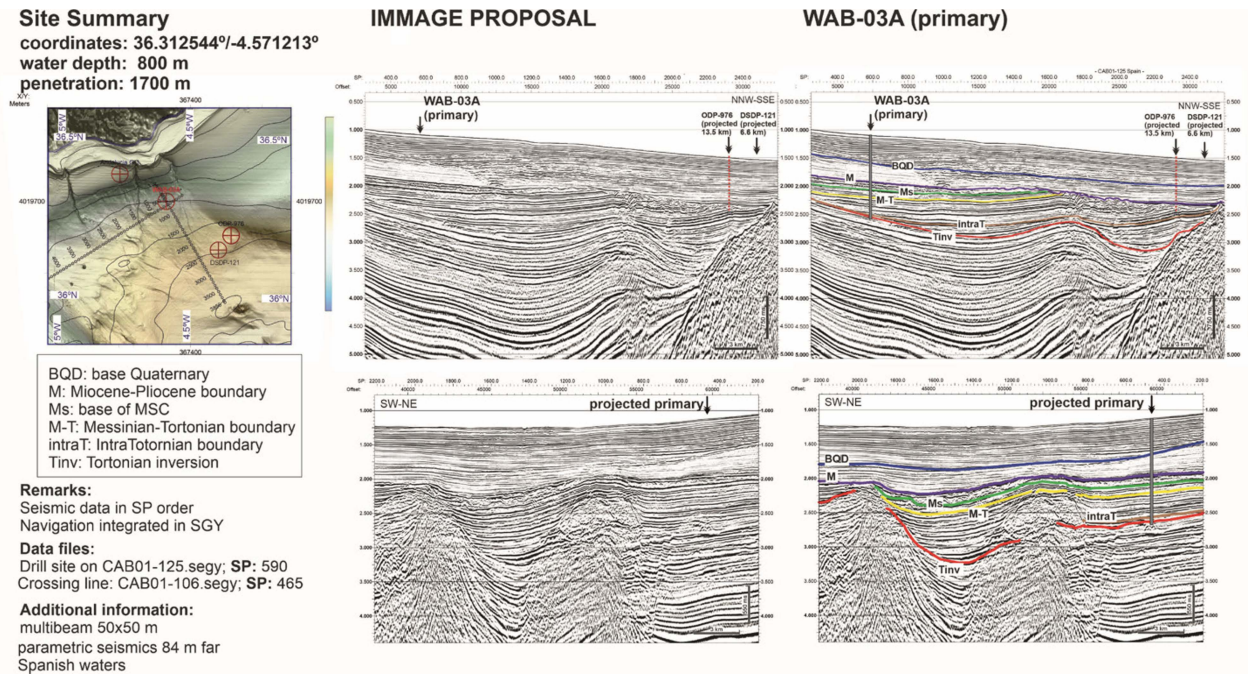

Figure F14. Site summary form for primary Site WAB-03A.

5.2.8. Site EAB-03A (alternate)

Site EAB-03A is at 838 mbsl (Figure F16). It also serves as an alternate site to Site WAB-03A and has the same objectives. It is very close to alternate Site EAB-02A. It is also close to ODP Sites 977–979. Stratigraphic limits, lithologies, and paleoenvironments are very similar to those estimated for Site EAB-02A. The Quaternary (0–2.6 My; 0–444 mbsf) and Pliocene (2.6–5.33/5.46 My; 444–711 mbsf) would be characterized by deep sea sedimentation and contourites with an average accumulation rate estimated to be ~150 m/My for the two periods. The Upper Miocene

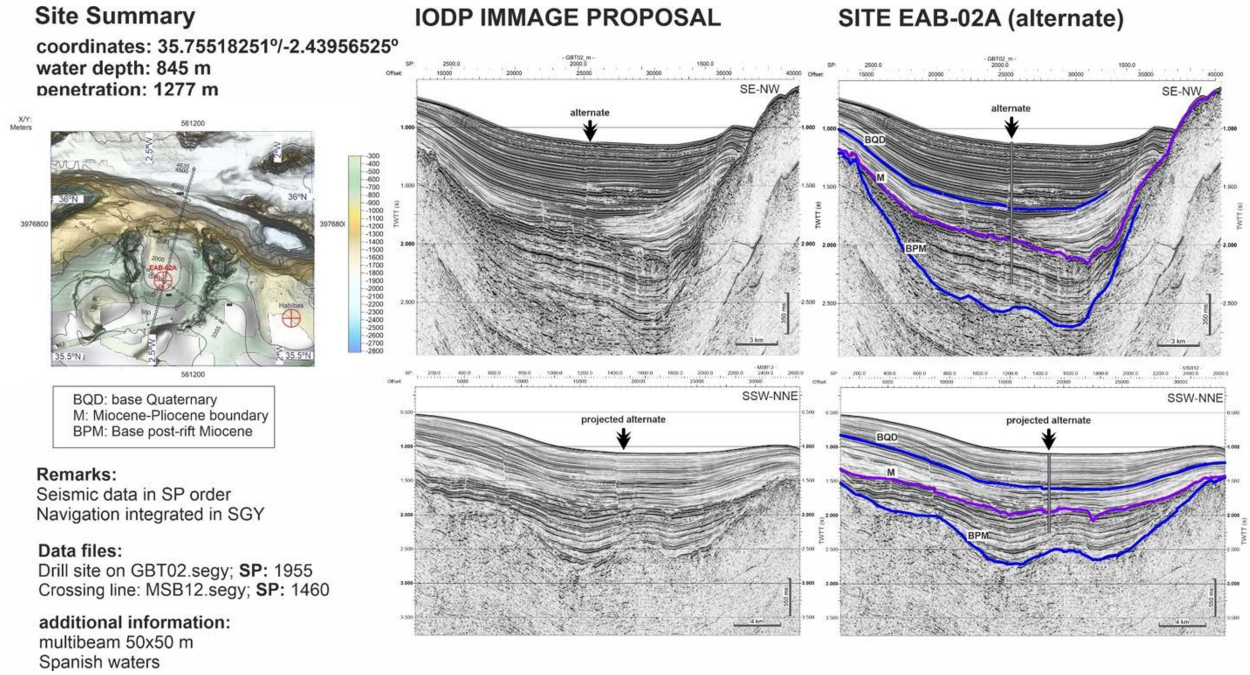

Figure F15. Site summary form for alternate Site EAB-02A.

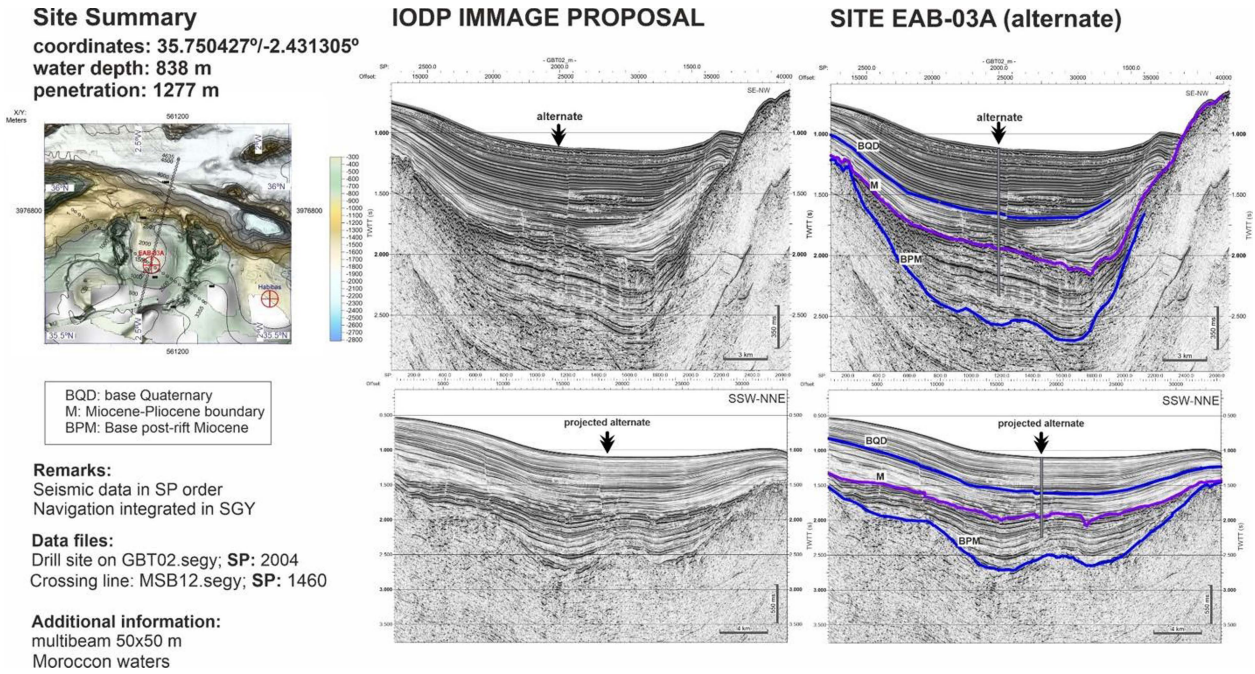

Figure F16. Site summary form for alternate Site EAB-03A.

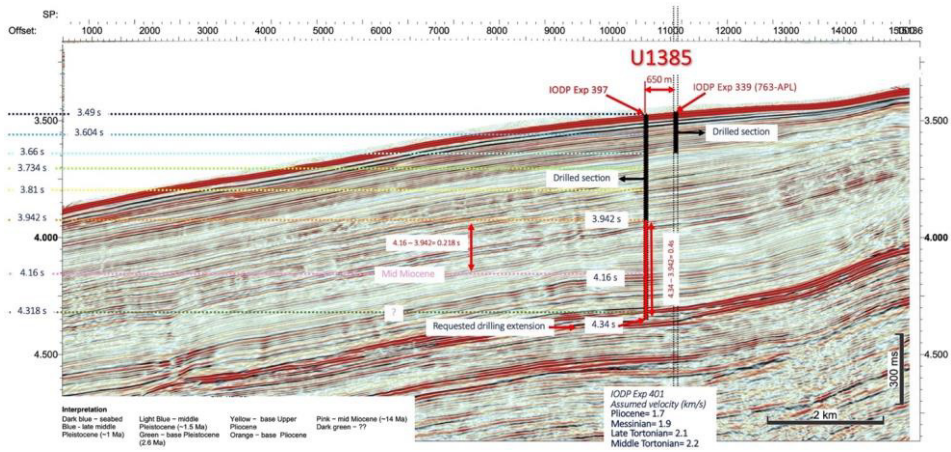

Figure F17. Seismic Line JC89-9 crossing Site U1385 and showing the drilled sections during Integrated Ocean Drilling Project Expeditions 339 and 397 and the requested extension to 4.34 s TWT. See Figure 12 in the Expedition 397 Scientific Prospectus (Hodell et al., 2022) for the cross line and site map.

(5.33/5.46 to <7.2 My; 711–1277 m) sedimentation would be subaerial/shallow waters during the MSC and open marine during the rest of the Miocene.

5.2.9. Site U1385 (alternate)

During Expedition 397, Site U1385 was cored to 400 mbsf (3.942 s TWT), the current EPSP depth limit, reaching ~4.5 Ma Early Pliocene strata. We are currently requesting permission to extend that drilling depth to a discontinuity located at 4.34 s TWT (dark green discontinuity, Figure **F17**) to recover the Late Miocene sequence of equivalent age to those targeted by the three primary Expedition 401 sites. We know that this succession exists at Site U1385 because the same Late Miocene sequence was recovered at Site U1587 downslope (Hodell et al., 2023) and this succession can be traced on the seismic between the two sites. The Late Miocene sediments at Site U1587 display very well developed precessional cyclicity. However, the poor carbonate preservation at this deeper water site (3480 m water depth) means that high-resolution carbonate-based proxy records cannot be generated. The shallow water depth of Site U1385 (2590 m water depth) means it is likely to have better carbonate preservation, making these essential proxy records viable.

If we choose to drill at Site U1385, we would wash down to 370 mbsf (just 30 m above 400 mbsf) and then recover a further 503 m (30 + 473 m) of sediment to reach the drilling target depth of 873 mbsf.

5.3. Formation temperature measurements

Formation temperature is part of the science objectives of the expedition. In APC holes, three or four temperature measurements will be taken with the advanced piston corer temperature (APCT-3) temperature probe, typically on Cores 4, 7, 10, and 13. If we do not core an APC hole at a site, we will attempt to deploy the sediment temperature pressure (SETP) probe at least once.

6. Wireline logging/downhole measurements strategy

Wireline logging in the deepest hole of each site includes three tool strings: the triple combo (natural gamma ray, density, PEF, porosity, electrical resistivity, and magnetic susceptibility tools); the Formation MicroScanner (FMS)-sonic (natural gamma ray, FMS image, and sonic velocity tools); and the Versatile Seismic Imager (VSI) check shot tool. The air gun operations required for the check shot survey require marine mammal observation and must be conducted during daylight hours. For more information on the logging tools, see **http://iodp.tamu.edu/tools**; **http://iodp.tamu.edu/tools/logging**.

7. Risks and contingency

We have identified the following potential risks associated with Expedition 401 and have mitigated them as much as possible.

7.1. Marine traffic

The Gulf of Cadiz and west Portugal represent busy areas for maritime traffic. Fortunately, the proposed IMMAGE sites are at a considerable distance from the Gibraltar Strait (the closest site is >50 nmi from the Gibraltar Strait), which represents the most problematic area in that respect. The other busy area is offshore southwest Portugal (in front of the Saint Vincent Cape; blue area in Figure **F18**), which is a traffic control navigation channel. The closest proposed site to this area is alternate Site ALM-02A, which is 2.7 nmi west of this area. The Alborán Sea is also a busy area for maritime traffic, but its main route is again a considerable distance from the selected sites.

Sites GUB-02A and GUB-03A are close to an area used for submarine exercises. We expect to have to inform the Spanish authorities in advance that *JOIDES Resolution* will be in this area and will likely be required to report its position during Expedition 401.

7.2. Overpressure and shallow gas

There are no acoustic anomalies suggesting the presence of shallow gas within the sediments targeted in the west Alborán Basin, and seabed sampling carried out by Conoco-Philips in October 2000 close to Site WAB-03 did not reveal any evidence of oil, gas, or gas hydrate in the top ~5 m of the sediment. Gas levels in the existing ODP and DSDP holes in the area never became hazardous, and ODP Sites 979 and 976 had normal headspace concentrations of biogenic methane.

No shallow gas has been reported in the area of the proposed sites on the Atlantic margin. However, both Repsol Oil Company and The National Office of Hydrocarbons and Mines (ONHYM) have drawn our attention to the potential for overpressured zones within the early Messinian turbiditic subsurface sediments. We have therefore investigated this thoroughly with the support of Repsol, Chariot, and ONHYM and are targeting sites that we and our colleagues in Repsol can demonstrate have negligible overpressuring or gas.

7.3. Storms

The scheduling of Expedition 401 during midwinter runs a heightened risk of disruption to the drilling program due to storms and associated heave. One possible contingency that could be enacted under the right circumstances, is to change the site order of drilling and drill the more

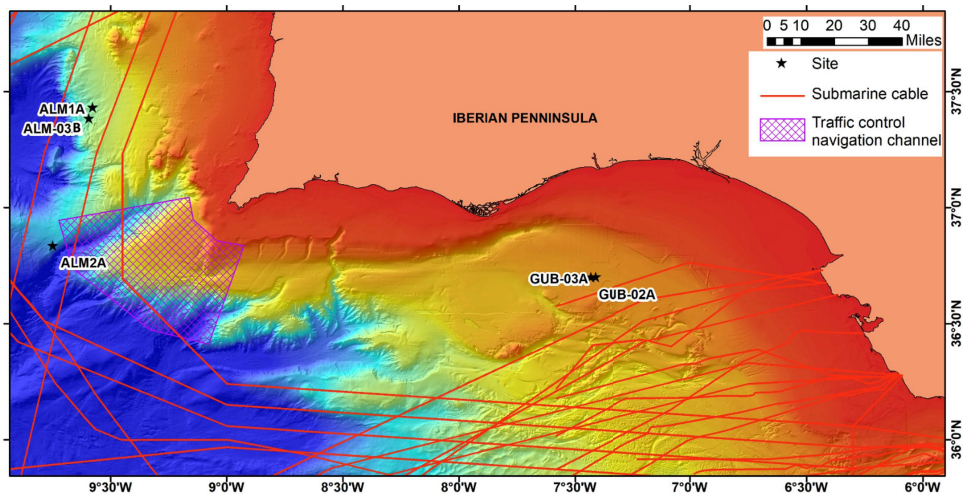

Figure F18. Position of Atlantic margin IODP sites for the IMMAGE project and adjacent submarine cables, pipelines, and traffic control navigation channels.

sheltered site within the Alborán Sea (WAB-03A) during a period where bad weather impacts the Atlantic. This would require additional time spent in transit (1–2 days).

7.4. Clearance

The drilling sites are in the Exclusive Economic Zones of Portugal and Spain, with two of the alternate sites in the Alborán Sea close to the Spanish/Moroccan border. Obtaining clearance to drill will be necessary.

7.5. COVID-19

COVID-19 continues to be a significant risk, and contingency plans are in place for a reduced science and technical party should conditions warrant. It may involve reduced core processing and analysis during the expedition with a shift toward increased shore-based activities during and/or after the expedition.

8. Sampling and data sharing strategy

As the first Land-2-Sea drilling project to be scheduled, it is possible that the standard IODP processes and protocols may need to be modified to ensure that the scientific objectives that straddle both the offshore and onshore cores are achieved. For example, because Expedition 401 is scheduled before either of the two onshore ICDP drilling campaigns, it is essential that sufficient Expedition 401 material is preserved to allow strategic sampling of the same intervals in both onshore and offshore cores. It is also worth noting that because Expedition 401 will recover only single records at each of its three sites, sample abundance may be restricted both during and after the moratorium period.

Shipboard and shore-based researchers should refer to the IODP Samples, Data, and Obligations Policy and Implementation Guidelines (**http://www.iodp.org/top-resources/program-documents/policies-and-guidelines**). This document outlines the policy for distributing IODP samples and data. It also defines the obligations incurred by sample and data recipients. The Sample Allocation Committee (SAC; composed of Co-Chief Scientists, Staff Scientist, and IODP Curator on shore and curatorial representative on board the ship) will work with the entire scientific party to formulate a formal expedition-specific sampling plan for shipboard and postcruise sampling.

Every member of the science party is obligated to carry out scientific research for the expedition and publish the results. Shipboard scientists are expected to submit sample requests (at **http://iodp.tamu.edu/curation/samples.html**) ~4 months before the beginning of the expedition. Based on sample requests (shore based and shipboard) submitted by this deadline, the SAC will prepare a tentative sampling plan, which will be revised on the ship as dictated by core recovery and cruise objectives. The sampling plan will be subject to modification depending upon the actual material recovered and collaborations that may evolve between scientists during the expedition. Modification of the strategy during the expedition must be approved by the Co-Chief Scientists, Staff Scientist, and curatorial representative on board the ship.

Given the specific objectives of Expedition 401, great care will be taken to maximize shared sampling to promote integration of data sets and enhance scientific collaboration among members of the scientific party so that IMMAGE's scientific Land-2-Sea objectives are met and each scientist has the opportunity to contribute. All sample sizes and frequencies must be justified on a scientific basis and will depend on core recovery, the full spectrum of other requests, and the expedition objectives. Some redundancy of measurement is unavoidable, but minimizing the duplication of measurements among the shipboard party and identified shore-based collaborators will be a factor in evaluating sample requests. If critical intervals are recovered, there may be considerable demand for samples from a limited amount of cored material. These intervals may require special handling, a higher sampling density, reduced sample size, or continuous core sampling by a single investigator. A sampling plan coordinated by the SAC may be required before critical intervals are sampled. Success will require collaboration, integration of complementary data sets, and consistent methods of analysis. Substantial collaboration and cooperation are highly encouraged. The

SAC may require an additional formal sampling plan before critical intervals are sampled, and a special sampling plan will be developed to maximize scientific return and scientific participation and to preserve some material for future studies. The SAC can decide at any stage during the expedition or during the 1 y moratorium period which recovered intervals should be considered critical.

Shipboard sampling will be restricted to acquiring ephemeral data types, shipboard measurements, and low-resolution sampling (e.g., biostratigraphic sampling and toothpick-sized samples for bulk carbonate isotopes), mainly so that we can rapidly produce age model data critical to the overall objectives of the expedition and for planning for higher resolution sampling postcruise. Whole-round samples may be taken for interstitial water measurements and physical property measurements as dictated by the shipboard sampling plan that will be finalized during the first few days of the expedition. The majority of the sampling for postcruise research will be postponed until a shore-based sampling party that will be implemented approximately 4–6 months after the end of the expedition at the Bremen Core Repository (BCR) in Bremen, Germany. All shipboard and approved shore-based scientists, students, and collaborators will be invited to help collect the thousands of anticipated samples.

The data collected during the expedition will be used to produce age models for each site, which are critical to the overall objectives of the expedition and for planning for higher resolution sampling postexpedition. The minimum permanent archive will be the standard archive half of each core and will not be sampled on board the ship. Following the expedition, the IODP Curator will finalize the selection of archive halves designated as permanent over any intervals recovered from multiple holes at a site.

For all IMMAGE's onshore and offshore sites, a highly coordinated sampling effort will be undertaken to produce a multiproxy data set on samples from the same stratigraphic horizons with acute attention to resolution, replication, and time control. This strategy requires close coordination between shipboard and shore-based scientists associated with Expedition 401 as well as those undertaking the equivalent tasks on the two ICDP drilling campaigns in Spain and Morocco. IMMAGE participants will be involved in the planning process to develop a sampling scheme that meets the needs of all investigators and fulfills the Land-2-Sea science objectives that underpin the original IMMAGE proposal.

All data and samples collected during Expedition 401 will be protected by a 1 y postcruise moratorium, during which time data and samples are available only to the Expedition 401 Science Party and approved shore-based participants. This moratorium will extend 1 y following the completion of the sampling party.

9. Expedition scientists and scientific participants

The current list of participants for Expedition 401 can be found at **http://iodp.tamu.edu/scienceops/expeditions/mediterranean_atlantic_gateway_exchange.html**.

10. Acknowledgments

This Scientific Prospectus is based on the original IMMAGE Land-2-Sea drilling project submitted to both IODP and ICDP. Without the extensive contributions, support, and encouragement of the IMMAGE proponents, we would not be in a position to be undertaking this ground-breaking drilling project and its associated science. We have also benefited from the amazing support of IODP and ICDP staff in helping us steer this, the first Land-2-Sea drilling proposal, through each organization's processes. Our particular thanks go to Michiko Yamamoto of IODP and Uli Harms of ICDP for their endless patience and encouragement.

References

Alhammoud, B., Meijer, P.T., and Dijkstra, H.A., 2010. Sensitivity of Mediterranean thermohaline circulation to gateway depth: a model investigation. Paleoceanography, 25(2):PA2220. **https://doi.org/10.1029/2009PA001823**

Álvarez, M., Pérez, F.F., Shoosmith, D.R., and Bryden, H.L., 2005. Unaccounted role of Mediterranean water in the drawdown of anthropogenic carbon. Journal of Geophysical Research: Oceans, 110(C9):C09S03. **https://doi.org/10.1029/2004JC002633**

Bahr, A., Kaboth, S., Jiménez-Espejo, F.J., Sierro, F.J., Voelker, A.H.L., Lourens, L., Röhl, U., Reichart, G.J., Escutia, C., Hernández-Molina, F.J., Pross, J., and Friedrich, O., 2015. Persistent monsoonal forcing of Mediterranean Outflow Water dynamics during the late Pleistocene. Geology, 43(11):951–954. **https://doi.org/10.1130/G37013.1**

Benson, R.H., Rakic-El Bied, K., and Bonaduce, G., 1991. An important current reversal (influx) in the Rifian Corridor (Morocco) at the Tortonian-Messinian boundary: the end of Tethys Ocean. Paleoceanography, 6(1):165–192. **https://doi.org/10.1029/90PA00756**

Bigg, G.R., Jickells, T.D., Liss, P.S., and Osborn, T.J., 2003. The role of the oceans in climate. International Journal of Climatology, 23(10):1127–1159. **https://doi.org/10.1002/joc.926**

Bigg, G.R., and Wadley, M.R., 2001. Millennial-scale variability in the oceans: an ocean modelling view. Journal of Quaternary Science, 16(4):309–319. **https://doi.org/10.1002/jqs.599**

Blanc, P.-L., 2006. Improved modelling of the Messinian salinity crisis and conceptual implications. Palaeogeography, Palaeoclimatology, Palaeoecology, 238(1):349–372. **https://doi.org/10.1016/j.palaeo.2006.03.033**

Booth-Rea, G., R. Ranero, C., and Grevemeyer, I., 2018. The Alboran volcanic-arc modulated the Messinian faunal exchange and salinity crisis. Scientific Reports, 8(1):13015. **https://doi.org/10.1038/s41598-018-31307-7**

Borenäs, K.M., Wåhlin, A.K., Ambar, I., and Serra, N., 2002. The Mediterranean outflow splitting—a comparison between theoretical models and CANIGO data. Deep Sea Research, Part II: Topical Studies in Oceanography, 49(19):4195–4205. **https://doi.org/10.1016/S0967-0645(02)00150-9**

Broecker, W.S., 1991. The Great Ocean Conveyor. Oceanography, 4(2):79–89. **https://tos.org/oceanography/assets/docs/4-2_broecker.pdf**

Bryden, H.L., Candela, J., and Kinder, T.H., 1994. Exchange through the Strait of Gibraltar. Progress in Oceanography, 33(3):201–248. **https://doi.org/10.1016/0079-6611(94)90028-0**

Butzin, M., Lohmann, G., and Bickert, T., 2011. Miocene ocean circulation inferred from marine carbon cycle modeling combined with benthic isotope records. Paleoceanography, 26(1):PA1203. **https://doi.org/10.1029/2009PA001901**

Capella, W., Flecker, R., Hernández-Molina, F.J., Simon, D., Meijer, P.T., Rogerson, M., Sierro, F.J., and Krijgsman, W., 2019. Mediterranean isolation preconditioning the Earth sSystem for Late Miocene climate cooling. Scientific Reports, 9(1):3795. **https://doi.org/10.1038/s41598-019-40208-2**

Capella, W., Hernández-Molina, F.J., Flecker, R., Hilgen, F.J., Hssain, M., Kouwenhoven, T.J., van Oorschot, M., Sierro, F.J., Stow, D.A.V., Trabucho-Alexandre, J., Tulbure, M.A., de Weger, W., Yousfi, M.Z., and Krijgsman, W., 2017. Sandy contourite drift in the late Miocene Rifian Corridor (Morocco): Reconstruction of depositional environments in a foreland-basin seaway. Sedimentary Geology, 355:31-57. **https://www.sciencedirect.com/science/article/pii/S0037073817300957**

Cerling, T.E., Harris, J.M., MacFadden, B.J., Leakey, M.G., Quade, J., Eisenmann, V., and Ehleringer, J.R., 1997. Global vegetation change through the Miocene/Pliocene boundary. Nature, 389(6647):153–158. **https://doi.org/10.1038/38229**

Cullum, J., Stevens, D.P., and Joshi, M.M., 2016. Importance of ocean salinity for climate and habitability. Proceedings of the National Academy of Sciences of the United States of America, 113(16):4278–4283. **https://doi.org/10.1073/pnas.1522034113**

Diester-Haass, L., Billups, K., and Emeis, K.C., 2006. Late Miocene carbon isotope records and marine biological productivity: was there a (dusty) link? Paleoceanography, 21(4):PA4216. **https://doi.org/10.1029/2006PA001267**

Dietrich, D.E., Tseng, Y.-H., Medina, R., Piacsek, S.A., Liste, M., Olabarrieta, M., Bowman, M.J., and Mehra, A., 2008. Mediterranean Overflow Water (MOW) simulation using a coupled multiple-grid Mediterranean Sea/North Atlantic Ocean model. Journal of Geophysical Research: Oceans, 113(C7):C07027. **https://doi.org/10.1029/2006JC003914**

Dixon, R.K., Solomon, A.M., Brown, S., Houghton, R.A., Trexier, M.C., and Wisniewski, J., 1994. Carbon pools and flux of global forest ecosystems. Science, 263(5144):185–190. **https://doi.org/10.1126/science.263.5144.185**

Do Couto, D., Gorini, C., Jolivet, L., Lebret, N., Augier, R., Gumiaux, C., d'Acremont, E., Ammar, A., Jabour, H., and Auxietre, J.-L., 2016. Tectonic and stratigraphic evolution of the Western Alboran Sea Basin in the last 25 Myrs. Tectonophysics, 677–678:280–311. **https://doi.org/10.1016/j.tecto.2016.03.020**

Drury, A.J., Westerhold, T., Frederichs, T., Tian, J., Wilkens, R., Channell, J.E.T., Evans, H., John, C.M., Lyle, M., and Röhl, U., 2017. Late Miocene climate and time scale reconciliation: accurate orbital calibration from a deep-sea perspective. Earth and Planetary Science Letters, 475:254–266. **https://doi.org/10.1016/j.epsl.2017.07.038**

Duggen, S., Hoernle, K., van den Bogaard, P., Rüpke, L., and Phipps Morgan, J., 2003. Deep roots of the Messinian salinity crisis. Nature, 422(6932):602–606. **https://doi.org/10.1038/nature01553**

Dupont, L.M., Rommerskirchen, F., Mollenhauer, G., and Schefuß, E., 2013. Miocene to Pliocene changes in South African hydrology and vegetation in relation to the expansion of C_4 plants. Earth and Planetary Science Letters, 375:408–417. **https://doi.org/10.1016/j.epsl.2013.06.005**

Elsworth, G., Galbraith, E., Halverson, G., and Yang, S., 2017. Enhanced weathering and CO_2 drawdown caused by latest Eocene strengthening of the Atlantic meridional overturning circulation. Nature Geoscience, 10(3):213–216. **https://doi.org/10.1038/ngeo2888**

Estrada, F., Ercilla, G., Gorini, C., Alonso, B., Vázquez, J.T., García-Castellanos, D., Juan, C., Maldonado, A., Ammar, A., and Elabbassi, M., 2011. Impact of pulsed Atlantic water inflow into the Alboran Basin at the time of the Zanclean flooding. Geo-Marine Letters, 31(5):361–376. **https://doi.org/10.1007/s00367-011-0249-8**

Expedition 339 Scientists, 2013. Expedition 339 summary. In Stow, D.A.V., Hernández-Molina, F.J., Alvarez Zarikian, C.A., and the Expedition 339 Scientists, Proceedings of the Integrated Ocean Drilling Program. 339: Tokyo (Integrated Ocean Drilling Program Management International, Inc.). **https://doi.org/10.2204/iodp.proc.339.101.2013**

Faccenna, C., Piromallo, C., Crespo-Blanc, A., Jolivet, L., and Rossetti, F., 2004. Lateral slab deformation and the origin of the western Mediterranean arcs. Tectonics, 23(1):TC1012. **https://doi.org/10.1029/2002TC001488**

Flecker, R., Krijgsman, W., Capella, W., de Castro Martíns, C., Dmitrieva, E., Mayser, J.P., Marzocchi, A., Modestou, S., Ochoa, D., Simon, D., Tulbure, M., van den Berg, B., van der Schee, M., de Lange, G., Ellam, R., Govers, R., Gutjahr, M., Hilgen, F., Kouwenhoven, T., Lofi, J., Meijer, P., Sierro, F.J., Bachiri, N., Barhoun, N., Alami, A.C., Chacon, B., Flores, J.A., Gregory, J., Howard, J., Lunt, D., Ochoa, M., Pancost, R., Vincent, S., and Yousfi, M.Z., 2015. Evolution of the Late Miocene Mediterranean–Atlantic gateways and their impact on regional and global environmental change. Earth-Science Reviews, 150:365–392. **https://doi.org/10.1016/j.earscirev.2015.08.007**

Foster, G.L., Royer, D.L., and Lunt, D.J., 2017. Future climate forcing potentially without precedent in the last 420 million years. Nature Communications, 8(1):14845. **https://doi.org/10.1038/ncomms14845**

García-Gallardo, Á., Grunert, P., Van der Schee, M., Sierro, F.J., Jiménez-Espejo, F.J., Alvarez Zarikian, C.A., and Piller, W.E., 2017. Benthic foraminifera-based reconstruction of the first Mediterranean-Atlantic exchange in the early Pliocene Gulf of Cadiz. Palaeogeography, Palaeoclimatology, Palaeoecology, 472:93–107. **https://doi.org/10.1016/j.palaeo.2017.02.009**

García-Gallardo, Á., Grunert, P., Voelker, A.H.L., Mendes, I., and Piller, W.E., 2017. Re-evaluation of the "elevated epifauna" as indicator of Mediterranean outflow water in the Gulf of Cadiz using stable isotopes ($\delta^{13}C$, $\delta^{18}O$). Global and Planetary Change, 155:78–97. **https://doi.org/10.1016/j.gloplacha.2017.06.005**

Grant, K.M., Rohling, E.J., Westerhold, T., Zabel, M., Heslop, D., Konijnendijk, T., and Lourens, L., 2017. A 3 million year index for North African humidity/aridity and the implication of potential pan-African Humid periods. Quaternary Science Reviews, 171:100–118. **https://doi.org/10.1016/j.quascirev.2017.07.005**

Guerra-Merchán, A., Serrano, F., Garcés, M., Gofas, S., Esu, D., Gliozzi, E., and Grossi, F., 2010. Messinian Lago-Mare deposits near the Strait of Gibraltar (Malaga Basin, S Spain). Palaeogeography, Palaeoclimatology, Palaeoecology, 285(3):264–276. **https://doi.org/10.1016/j.palaeo.2009.11.019**

Gulick, S.P.S., Shevenell, A.E., Montelli, A., Fernandez, R., Smith, C., Warny, S., Bohaty, S.M., Sjunneskog, C., Leventer, A., Frederick, B., and Blankenship, D.D., 2017. Initiation and long-term instability of the East Antarctic Ice Sheet. Nature, 552(7684):225–229. **https://doi.org/10.1038/nature25026**

Herbert, T.D., Lawrence, K.T., Tzanova, A., Peterson, L.C., Caballero-Gill, R., and Kelly, C.S., 2016. Late Miocene global cooling and the rise of modern ecosystems. Nature Geoscience, 9(11):843–847. **https://doi.org/10.1038/ngeo2813**

Hernández-Molina, F.J., Llave, E., Preu, B., Ercilla, G., Fontan, A., Bruno, M., Serra, N., Gomiz, J.J., Brackenridge, R.E., Sierro, F.J., Stow, D.A.V., García, M., Juan, C., Sandoval, N., and Arnaiz, A., 2014a. Contourite processes associated with the Mediterranean Outflow Water after its exit from the Strait of Gibraltar: global and conceptual implications. Geology, 42(3):227–230. **https://doi.org/10.1130/G35083.1**

Hernández-Molina, F.J., Sierro, F.J., Llave, E., Roque, C., Stow, D.A.V., Williams, T., Lofi, J., Van der Schee, M., Arnáiz, A., Ledesma, S., Rosales, C., Rodríguez-Tovar, F.J., Pardo-Igúzquiza, E., and Brackenridge, R.E., 2016. Evolution of the Gulf of Cadiz margin and southwest Portugal contourite depositional system: tectonic, sedimentary and paleoceanographic implications from IODP Expedition 339. Marine Geology, 377:7–39. **https://doi.org/10.1016/j.margeo.2015.09.013**

Hernández-Molina, F.J., Stow, D.A.V., Alvarez-Zarikian, C.A., Acton, G., Bahr, A., Balestra, B., Ducassou, E., Flood, R., Flores, J.-A., Furota, S., Grunert, P., Hodell, D., Jimenez-Espejo, F., Kim, J.K., Krissek, L., Kuroda, J., Li, B., Llave, E., Lofi, J., Lourens, L., Miller, M., Nanayama, F., Nishida, N., Richter, C., Roque, C., Pereira, H., Sanchez Goñi, M.F., Sierro, F.J., Singh, A.D., Sloss, C., Takashimizu, Y., Tzanova, A., Voelker, A., Williams, T., and Xuan, C., 2014b. Onset of Mediterranean outflow into the North Atlantic. Science, 344(6189):1244–1250. **https://doi.org/10.1126/science.1251306**

Hernández-Molina, J., Llave, E., Somoza, L., Fernández-Puga, M.C., Maestro, A., León, R., Medialdea, T., Barnolas, A., García, M., Díaz del Río, V., Fernández-Salas, L.M., Vázquez, J.T., Lobo, F., Alveirinho Dias, J.M., Rodero, J., and Gardner, J., 2003. Looking for clues to paleoceanographic imprints: a diagnosis of the Gulf of Cadiz contourite depositional systems. Geology, 31(1):19–22. **https://doi.org/10.1130/0091-7613(2003)031%3C0019:LFCTPI%3E2.0.CO;2**

Hilgen, F., Aziz, H.A., Bice, D., Iaccarino, S., Krijgsman, W., Kuiper, K., Montanari, A., Raffi, I., Turco, E., and Zachariasse, W.-J., 2005. The global boundary stratotype section and point (GSSP) of the Tortonian Stage (Upper Miocene) at Monte Dei Corvi. International Union of Geological Sciences, 28(1):6–17. **https://doi.org/10.18814/epiiugs/2005/v28i1/001**

Hilgen, F.J., Kuiper, K.F., Krijgsman, W., Snel, E., and Laan, E.v.d., 2007. Astronomical tuning as the basis for high resolution chronostratigraphy: the intricate history of the Messinian Salinity Crisis. Newsletters on Stratigraphy, 4(2–3):231–238.

Hodell, D.A., Abrantes, F., and Alvarez Zarikian, C.A., 2022. Expedition 397 Scientific Prospectus: Iberian Margin Paleoclimate. International Ocean Discovery Program. **https://doi.org/10.14379/iodp.sp.397.2022**

Hodell, D.A., Abrantes, F., Alvarez Zarikian, C.A., and the Expedition 397 Scientists, 2023. Expedition 397 Preliminary Report: Iberian Margin Paleoclimate. International Ocean Discovery Program. **https://doi.org/10.14379/iodp.pr.397.2023**

Hodell, D.A., Curtis, J.H., Sierro, F.J., and Raymo, M.E., 2001. Correlation of Late Miocene to Early Pliocene sequences between the Mediterranean and North Atlantic. Paleoceanography, 16(2):164–178. **https://doi.org/10.1029/1999PA000487**

Hodell, D.A., and Venz-Curtis, K.A., 2006. Late Neogene history of deepwater ventilation in the Southern Ocean. Geochemistry, Geophysics, Geosystems, 7(9):Q09001. **https://doi.org/10.1029/2005GC001211**

Hsü, K.J., Ryan, W.B.F., and Cita, M.B., 1973. Late Miocene desiccation of the Mediterranean. Nature, 242(5395):240–244. **https://doi.org/10.1038/242240a0**

Iaccarino, S.M., and Bossio, A., 1999. Paleoenvironment of uppermost Messinian sequences in the western Mediterranean (Sites 974, 975, and 978). In Zahn, R., Comas, M.C., and Klaus, A. (Eds.), Proceedings of the Ocean Drilling Program, Scientific Results. 161: College Station, TX (Ocean Drilling Program). **https://doi.org/10.2973/odp.proc.sr.161.246.1999**

Intergovernmental Panel on Climate Change, 2014. Climate Change 2013 – The Physical Science Basis: Cambridge, UK (Cambridge University Press). **https://www.cambridge.org/core/books/climate-change-2013-the-physical-science-basis/BE9453E500DEF3640B383BADDC332C3E**

Iorga, M.C., and Lozier, M.S., 1999. Signatures of the Mediterranean outflow from a North Atlantic climatology: 1. Salinity and density fields. Journal of Geophysical Research: Oceans, 104(C11):25985–26009. **https://doi.org/10.1029/1999JC900115**

Ivanovic, R.F., Valdes, P.J., Flecker, R., Gregoire, L.J., and Gutjahr, M., 2013. The parameterisation of Mediterranean–Atlantic water exchange in the Hadley Centre model HadCM3, and its effect on modelled North Atlantic climate. Ocean Modelling, 62:11–16. **https://doi.org/10.1016/j.ocemod.2012.11.002**

Ivanovic, R.F., Valdes, P.J., Flecker, R., and Gutjahr, M., 2014a. Modelling global-scale climate impacts of the late Miocene Messinian salinity crisis. Climate of the Past, 10(2):607–622. **https://doi.org/10.5194/cp-10-607-2014**

Ivanovic, R.F., Valdes, P.J., Gregoire, L., Flecker, R., and Gutjahr, M., 2014b. Sensitivity of modern climate to the presence, strength and salinity of Mediterranean-Atlantic exchange in a global general circulation model. Climate Dynamics, 42(3):859–877. **https://doi.org/10.1007/s00382-013-1680-5**

Jolivet, L., and Faccenna, C., 2000. Mediterranean extension and the Africa-Eurasia collision. Tectonics, 19(6):1095–1106. **https://doi.org/10.1029/2000TC900018**

Juan, C., Ercilla, G., Estrada, F., Alonso, B., Casas, D., Vázquez, J.T., d'Acremont, E., Medialdea, T., Hernández-Molina, F.J., Gorini, C., El Moumni, B., and Valencia, J., 2020. Multiple factors controlling the deep marine sedimentation of the Alboran Sea (SW Mediterranean) after the Zanclean Atlantic mega-flood. Marine Geology, 423:106138. **https://doi.org/10.1016/j.margeo.2020.106138**

Juan, C., Ercilla, G., Javier Hernández-Molina, F., Estrada, F., Alonso, B., Casas, D., García, M., Farran, M.l., Llave, E., Palomino, D., Vázquez, J.-T., Medialdea, T., Gorini, C., D'Acremont, E., El Moumni, B., and Ammar, A., 2016. Seismic evidence of current-controlled sedimentation in the Alboran Sea during the Pliocene and Quaternary: palaeoceanographic implications. Marine Geology, 378:292–311. **https://doi.org/10.1016/j.margeo.2016.01.006**

Kaboth-Bahr, S., Bahr, A., Zeeden, C., Toucanne, S., Eynaud, F., Jiménez-Espejo, F., Röhl, U., Friedrich, O., Pross, J., Löwemark, L., and Lourens, L.J., 2018. Monsoonal forcing of European ice-sheet dynamics during the late Quaternary. Geophysical Research Letters, 45(14):7066–7074. **https://doi.org/10.1029/2018GL078751**

Kaminski, M.A., Aksu, A., Box, M., Hiscott, R.N., Filipescu, S., and Al-Salameen, M., 2002. Late Glacial to Holocene benthic foraminifera in the Marmara Sea: implications for Black Sea–Mediterranean Sea connections following the last deglaciation. Marine Geology, 190(1):165–202. **https://doi.org/10.1016/S0025-3227(02)00347-X**

Karas, C., Nürnberg, D., Bahr, A., Groeneveld, J., Herrle, J.O., Tiedemann, R., and deMenocal, P.B., 2017. Pliocene oceanic seaways and global climate. Scientific Reports, 7(1):39842. **https://doi.org/10.1038/srep39842**

Kennett, J.P., 1982. Marine Geology: Englewood Cliffs, NJ (Prentice-Hall).

Khélifi, N., Sarnthein, M., Andersen, N., Blanz, T., Frank, M., Garbe-Schönberg, D., Haley, B.A., Stumpf, R., and Weinelt, M., 2009. A major and long-term Pliocene intensification of the Mediterranean outflow, 3.5–3.3 Ma ago. Geology, 37(9):811–814. **https://doi.org/10.1130/G30058A.1**

Knutz, P.C., 2008. Palaeoceanographic significance of contourite drifts. In Rebesco, M., and Camerlenghi, A. (Eds.), Contourites. Developments in Sedimentology, 60: (Elsevier), 511–535. **https://doi.org/10.1016/S0070-4571(08)10024-3**

Krijgsman, W., Capella, W., Simon, D., Hilgen, F.J., Kouwenhoven, T.J., Meijer, P.T., Sierro, F.J., Tulbure, M.A., van den Berg, B.C.J., van der Schee, M., and Flecker, R., 2018. The Gibraltar Corridor: Watergate of the Messinian Salinity Crisis. Marine Geology, 403:238–246. **https://doi.org/10.1016/j.margeo.2018.06.008**

Krijgsman, W., Hilgen, F.J., Raffi, I., Sierro, F.J., and Wilson, D.S., 1999. Chronology, causes and progression of the Messinian salinity crisis. Nature, 400(6745):652–655. **https://doi.org/10.1038/23231**

LaRiviere, J.P., Ravelo, A.C., Crimmins, A., Dekens, P.S., Ford, H.L., Lyle, M., and Wara, M.W., 2012. Late Miocene decoupling of oceanic warmth and atmospheric carbon dioxide forcing. Nature, 486(7401):97–100. **https://doi.org/10.1038/nature11200**

Larsen, H.C., Saunders, A.D., Clift, P.D., Beget, J., Wei, W., and Spezzaferri, S., 1994. Seven million years of glaciation in Greenland. Science, 264(5161):952–955. **https://doi.org/10.1126/science.264.5161.952**

Ledesma, S., 2000. Astrobiocronología y Estratigrafía de Alta Resolución del Neógeno de la Cuenca del Guadalquivir-Golfo de Cadiz [PhD dissertation]. University of Salamanca, Salamanca, Spain.

Legg, S., Briegleb, B., Chang, Y., Chassignet, E.P., Danabasoglu, G., Ezer, T., Gordon, A.L., Griffies, S., Hallberg, R., Jackson, L., Large, W., Özgökmen, T.M., Peters, H., Price, J., Riemenschneider, U., Wu, W., Xu, X., and Yang, J., 2009. Improving oceanic overflow representation in climate models: the gravity current entrainment climate pro-

cess team. Bulletin of the American Meteorological Society, 90(5):657–670. **https://doi.org/10.1175/2008BAMS2667.1**

Lisiecki, L.E., and Raymo, M.E., 2005. A Pliocene-Pleistocene stack of 57 globally distributed benthic $\delta^{18}O$ records. Paleoceanography, 20(1):PA1003. **https://doi.org/10.1029/2004PA001071**

Lourens, L.J., Antonarakou, A., Hilgen, F.J., Van Hoof, A.A.M., Vergnaud-Grazzini, C., and Zachariasse, W.J., 1996. Evaluation of the Plio-Pleistocene astronomical timescale. Paleoceanography, 11(4):391–413. **https://doi.org/10.1029/96PA01125**

Manzi, V., Gennari, R., Hilgen, F., Krijgsman, W., Lugli, S., Roveri, M., and Sierro, F.J., 2013. Age refinement of the Messinian salinity crisis onset in the Mediterranean. Terra Nova, 25(4):315–322. **https://doi.org/10.1111/ter.12038**

Martín, J.M., Braga, J.C., Aguirre, J., and Puga-Bernabéu, Á., 2009. History and evolution of the North-Betic Strait (Prebetic Zone, Betic Cordillera): a narrow, early Tortonian, tidal-dominated, Atlantic–Mediterranean marine passage. Sedimentary Geology, 216(3):80–90. **https://doi.org/10.1016/j.sedgeo.2009.01.005**

Marzocchi, A., 2016. Modelling the impact of orbital forcing on Late Miocene climate: implications for the Mediterranean Sea and the Messinian Salinity Crisis [PhD dissertation]. National Oceanography Centre, Southampton, England. **http://dx.doi.org/10.13140/RG.2.2.32943.12967**

Marzocchi, A., Lunt, D.J., Flecker, R., Bradshaw, C.D., Farnsworth, A., and Hilgen, F.J., 2015. Orbital control on Late Miocene climate and the North African monsoon: insight from an ensemble of sub-precessional simulations. Climate of the Past, 11(10):1271–1295. **https://doi.org/10.5194/cp-11-1271-2015**

Medaouri, M., Déverchère, J., Graindorge, D., Bracene, R., Badji, R., Ouabadi, A., Yelles-Chaouche, K., and Bendiab, F., 2014. The transition from Alboran to Algerian basins (Western Mediterranean Sea): chronostratigraphy, deep crustal structure and tectonic evolution at the rear of a narrow slab rollback system. Journal of Geodynamics, 77:186–205. **https://doi.org/10.1016/j.jog.2014.01.003**

Mercer, J.H., and Sutter, J.F., 1982. Late Miocene—Earliest Pliocene glaciation in southern Argentina: implications for global ice-sheet history. Palaeogeography, Palaeoclimatology, Palaeoecology, 38(3):185–206. **https://doi.org/10.1016/0031-0182(82)90003-7**

Modestou, S., Simon, D., Gutjahr, M., Marzocchi, A., Kouwenhoven, T.J., Ellam, R.M., and Flecker, R., 2017. Precessional variability of $^{87}Sr/^{86}Sr$ in the Late Miocene Sorbas Basin: an interdisciplinary study of drivers of interbasin exchange. Paleoceanography, 32(6):531–552. **https://doi.org/10.1002/2016PA003061**

Nelson, C.H., Baraza, J., Maldonado, A., Rodero, J., Escutia, C., and Barber Jr, J.H., 1999. Influence of the Atlantic inflow and Mediterranean outflow currents on late Quaternary sedimentary facies of the Gulf of Cadiz continental margin. Marine Geology, 155(1–2):99–129. **https://doi.org/10.1016/S0025-3227(98)00143-1**

Orszag-Sperber, F., 2006. Changing perspectives in the concept of "Lago-Mare" in Mediterranean Late Miocene evolution. Sedimentary Geology, 188–189:259–277. **https://doi.org/10.1016/j.sedgeo.2006.03.008**

Panitz, S., Salzmann, U., Risebrobakken, B., De Schepper, S., Pound, M.J., Haywood, A.M., Dolan, A.M., and Lunt, D.J., 2018. Orbital, tectonic and oceanographic controls on Pliocene climate and atmospheric circulation in Arctic Norway. Global and Planetary Change, 161:183–193. **https://doi.org/10.1016/j.gloplacha.2017.12.022**

Peixoto, J.P., and Kettani, M.A., 1973. The control of the water cycle. Scientific American, 228(4):46–63. **http://www.jstor.org/stable/24923025**

Penaud, A., Eynaud, F., Sánchez-Goñi, M., Malaizé, B., Turon, J.L., and Rossignol, L., 2011. Contrasting sea-surface responses between the western Mediterranean Sea and eastern subtropical latitudes of the North Atlantic during abrupt climatic events of MIS 3. Marine Micropaleontology, 80(1):1–17. **https://doi.org/10.1016/j.marmicro.2011.03.002**

Price, J.F., Baringer, M.O.N., Lueck, R.G., Johnson, G.C., Ambar, I., Parrilla, G., Cantos, A., Kennelly, M.A., and Sanford, T.B., 1993. Mediterranean Outflow mixing and dynamics. Science, 259(5099):1277–1282. **https://doi.org/10.1126/science.259.5099.1277**

Price, J.F., and O'Neil Baringer, M., 1994. Outflows and deep water production by marginal seas. Progress in Oceanography, 33(3):161–200. **https://doi.org/10.1016/0079-6611(94)90027-2**

Rahmstorf, S., 2006. Thermohaline ocean circulation. In Elias, S.A., Encyclopedia of Quaternary Sciences. Amsterdam (Elsevier), 739–750.

Rogerson, M., Bigg, G.R., Rohling, E.J., and Ramirez, J., 2012a. Vertical density gradient in the eastern North Atlantic during the last 30,000 years. Climate Dynamics, 39(3):589–598. **https://doi.org/10.1007/s00382-011-1148-4**

Rogerson, M., Colmenero-Hidalgo, E., Levine, R.C., Rohling, E.J., Voelker, A.H.L., Bigg, G.R., Schönfeld, J., Cacho, I., Sierro, F.J., Löwemark, L., Reguera, M.I., de Abreu, L., and Garrick, K., 2010. Enhanced Mediterranean-Atlantic exchange during Atlantic freshening phases. Geochemistry, Geophysics, Geosystems, 11(8):Q08013. **https://doi.org/10.1029/2009GC002931**

Rogerson, M., Rohling, E.J., Bigg, G.R., and Ramirez, J., 2012b. Paleoceanography of the Atlantic-Mediterranean exchange: overview and first quantitative assessment of climatic forcing. Reviews of Geophysics, 50(2):RG2003. **https://doi.org/10.1029/2011RG000376**

Rogerson, M., Rohling, E.J., and Weaver, P.P.E., 2006. Promotion of meridional overturning by Mediterranean-derived salt during the last deglaciation. Paleoceanography, 21(4):PA4101. **https://doi.org/10.1029/2006PA001306**

Rohling, E.J., 2007. Progress in paleosalinity: overview and presentation of a new approach. Paleoceanography, 22(3):PA3215. **https://doi.org/10.1029/2007PA001437**

Rouchy, J.M., Caruso, A., Pierre, C., Blanc-Valleron, M.-M., and Bassetti, M.A., 2007. The end of the Messinian salinity crisis: evidences from the Chelif Basin (Algeria). Palaeogeography, Palaeoclimatology, Palaeoecology, 254(3):386–417. **https://doi.org/10.1016/j.palaeo.2007.06.015**

Roveri, M., Flecker, R., Krijgsman, W., Lofi, J., Lugli, S., Manzi, V., Sierro, F.J., Bertini, A., Camerlenghi, A., De Lange, G., Govers, R., Hilgen, F.J., Hübscher, C., Meijer, P.T., and Stoica, M., 2014. The Messinian salinity crisis: past and future of a great challenge for marine sciences. Marine Geology, 352:25–58. **https://doi.org/10.1016/j.margeo.2014.02.002**

Ryan, W.B.F., Hsü, K.J., et al., 1973. Initial Reports of the Deep Sea Drilling Project, 13: Washington, DC (US Government Printing Office). **https://doi.org/10.2973/dsdp.proc.13.1973**

Siegenthaler, U., and Sarmiento, J.L., 1993. Atmospheric carbon dioxide and the ocean. Nature, 365(6442):119–125. **https://doi.org/10.1038/365119a0**

Smethie, W.M., Jr., Fine, R.A., Putzka, A., and Jones, E.P., 2000. Tracing the flow of North Atlantic Deep Water using chlorofluorocarbons. Journal of Geophysical Research: Oceans, 105(C6):14297–14323. **https://doi.org/10.1029/1999JC900274**

Smith, A.G., and Pickering, K.T., 2003. Oceanic gateways as a critical factor to initiate icehouse Earth. Journal of the Geological Society, 160(3):337–340. **https://doi.org/10.1144/0016-764902-115**

St. John, K.E.K., and Krissek, L.A., 2002. The Late Miocene to Pleistocene ice-rafting history of southeast Greenland. Boreas, 31(1):28–35. **https://doi.org/10.1111/j.1502-3885.2002.tb01053.x**

Stanley, D.J., 1975. Messinian events in the Mediterranean: C. W. Drooger (editor). North-Holland, Amsterdam, 1973, 272 pp., Dfl. 60.00. Marine Geology, 18(5):339–342. **https://doi.org/10.1016/0025-3227(75)90028-6**

Tans, P.P., Berry, J.A., and Keeling, R.F., 1993. Oceanic $^{13}C/^{12}C$ observations: a new window on ocean CO_2 uptake. Global Biogeochemical Cycles, 7(2):353–368. **https://doi.org/10.1029/93GB00053**

Taylforth, J.E., McCay, G.A., Ellam, R., Raffi, I., Kroon, D., and Robertson, A.H.F., 2014. Middle Miocene (Langhian) sapropel formation in the easternmost Mediterranean deep-water basin: evidence from northern Cyprus. Marine and Petroleum Geology, 57:521–536. **https://doi.org/10.1016/j.marpetgeo.2014.04.015**

Thomas, H., Bozec, Y., Elkalay, K., and de Baar, H.J.W., 2004. Enhanced open ocean storage of CO_2 from shelf sea pumping. Science, 304(5673):1005–1008. **https://doi.org/10.1126/science.1095491**

van der Laan, E., Hilgen, F.J., Lourens, L.J., de Kaenel, E., Gaboardi, S., and Iaccarino, S., 2012. Astronomical forcing of Northwest African climate and glacial history during the late Messinian (6.5–5.5Ma). Palaeogeography, Palaeoclimatology, Palaeoecology, 313–314:107–126. **https://doi.org/10.1016/j.palaeo.2011.10.013**

van der Laan, E., Snel, E., de Kaenel, E., Hilgen, F.J., and Krijgsman, W., 2006. No major deglaciation across the Miocene-Pliocene boundary: integrated stratigraphy and astronomical tuning of the Loulja sections (Bou Regreg area, NW Morocco). Paleoceanography, 21(3):PA3011. **https://doi.org/10.1029/2005PA001193**

van der Schee, M., Sierro, F.J., Jiménez-Espejo, F.J., Hernández-Molina, F.J., Flecker, R., Flores, J.A., Acton, G., Gutjahr, M., Grunert, P., Garcia-Gallardo, A., and Andersen, N., 2016. Evidence of early bottom water current flow after the Messinian Salinity Crisis in the Gulf of Cadiz. Marine Geology, 380:315–329. **https://doi.org/10.1016/j.margeo.2016.04.005**

van Hinsbergen, D.J.J., Vissers, R.L.M., and Spakman, W., 2014. Origin and consequences of western Mediterranean subduction, rollback, and slab segmentation. Tectonics, 33(4):393–419. **https://doi.org/10.1002/2013TC003349**

Voelker, A.H.L., Lebreiro, S.M., Schönfeld, J., Cacho, I., Erlenkeuser, H., and Abrantes, F., 2006. Mediterranean outflow strengthening during northern hemisphere coolings: a salt source for the glacial Atlantic? Earth and Planetary Science Letters, 245(1):39–55. **https://doi.org/10.1016/j.epsl.2006.03.014**

Williams, T., van de Flierdt, T., Hemming, S.R., Chung, E., Roy, M., and Goldstein, S.L., 2010. Evidence for iceberg armadas from East Antarctica in the Southern Ocean during the Late Miocene and Early Pliocene. Earth and Planetary Science Letters, 290(3–4):351–361. **https://doi.org/10.1016/j.epsl.2009.12.031**

Zachos, J.C., Dickens, G.R., and Zeebe, R.E., 2008. An early Cenozoic perspective on greenhouse warming and carbon-cycle dynamics. Nature, 451(7176):279–283. **https://doi.org/10.1038/nature06588**

Zachos, J.C., Shackleton, N.J., Revenaugh, J.S., Pälike, H., and Flower, B.P., 2001. Climate response to orbital forcing across the Oligocene-Miocene boundary. Science, 292(5515):274–278. **https://doi.org/10.1126/science.1058288**

Zhang, Z., Ramstein, G., Schuster, M., Li, C., Contoux, C., and Yan, Q., 2014. Aridification of the Sahara desert caused by Tethys Sea shrinkage during the Late Miocene. Nature, 513(7518):401–404. **https://doi.org/10.1038/nature13705**

Site summaries

Site ALM-03B

Priority:	Primary
Position:	37.37711°N, 9.59853°W
Water depth (m):	1634
Target drilling depth (mbsf):	930
Approved maximum penetration (mbsf):	930
Survey coverage (track map; seismic profile):	Inline: WPortugal_IL1740_ALM03B.sgy Position: CDP CDP1740 Crossline: WPortugal_XL5210_ALM03B.sgy Position: CDP CDP5210
Objectives:	• Recover a thick, shallow Late Miocene succession which contains distal Mediterranean overflow deposits • Test quantitative constraints on the behavior of sense overflows (Objective 3) • Recover the high resolution (precessional) record of Mediterranean–Atlantic exchange during Late Miocene-Pliocene (Objectives 1 and 2)
Coring program:	See text
Downhole measurements program:	Triple combo tool string, FMS-sonic, VSP
Nature of rock anticipated:	Muds, muddy sands, sands

Site GUB-02A

Priority:	Primary
Position:	36.699683°N, 7.431424°W
Water depth (m):	547
Target drilling depth (mbsf):	1464
Approved maximum penetration (mbsf):	1464 (approved by EPSP on 31 March 2023)
Survey coverage (track map; seismic profile):	Inline: GulfofCadiz_IL3170_GUB02A.sgy Position: CDP CDP939 Crossline: GulfofCadiz_XL2125_GUB02A.sgy Position: CDP CDP2189
Objectives:	• Recover a complete Late Miocene succession in the pathway of Mediterranean overflow • Obtain a high-resolution (precessional) record of Miocene Mediterranean overflow at an intermediate site between the onshore records (RIF-01A and BET-01A) and the distal record (ALM-03A) (Objectives 1, 2 and 3)
Coring program:	See text
Downhole measurements program:	Triple combo tool string, FMS-sonic, VSP
Nature of rock anticipated:	Muds, muddy sands, marls, sands

Site WAB-03A

Priority:	Primary
Position:	36.312544°N, 4.571213°W
Water depth (m):	800
Target drilling depth (mbsf):	1700
Approved maximum penetration (mbsf):	1700
Survey coverage (track map; seismic profile):	Inline: CAB01-125 Position: SP 590 Crossline: CAB01-106 Position: SP 472
Objectives:	• Recover one of the few thick Late Messinian sedimentary successions in the Alboran Basin • Obtain key contraints on the chemistry and physical properties of Mediterranean overflow during the Late Miocene (Objectives 1, 2 and 3)
Coring program:	See text
Downhole measurements program:	Triple combo tool string, FMS-sonic, VSP
Nature of rock anticipated:	Conglomerates, sandstones, marles, shales, volcanoclastics, clays, minor anhydrite/gypsum

Site ALM-01A

Priority:	Alternate
Position:	37.4317°N, 9.5767°W
Water depth (m):	1567
Target drilling depth (mbsf):	990
Approved maximum penetration (mbsf):	990
Survey coverage (track map; seismic profile):	Inline: PD00522_ALM-1A_WPORTUGAL Position: SHOT POINT 4340 Crossline: PD00610_ALM-1A_WPORTUGAL
Objectives:	• Recover a thick, shallow Late Miocene succession which contains distal Mediterranean overflow deposits • Test quantitative constraints on the behavior of sense overflows (Objective 3) • Recover the high resolution (precessional) recod of Mediterranean–Atlantic exchange during Late Miocene-Pliocene (Objectives 1 and 2)
Coring program:	See text
Downhole measurements program:	Triple combo tool string, FMS-sonic, VSP
Nature of rock anticipated:	Muds, muddy sands, marls

Site ALM-02A

Priority:	Alternate
Position:	36.8359°N, 9.7481°W
Water depth (m):	2265
Target drilling depth (mbsf):	1630
Approved maximum penetration (mbsf):	1630
Survey coverage (track map; seismic profile):	Inline: PD00608A_ALM-1B_WPORTUGAL Position: SP 10685 Crossline: PD00538_ALM-2A_WPORTUGAL
Objectives:	• Recover a thick, shallow Late Miocene succession which contains distal Mediterranean overflow deposits • Test quantitative constraints on the behavior of sense overflows (Objective 3) • Recover the high resolution (precessional) recod of Mediterranean–Atlantic exchange during Late Miocene-Pliocene (Objectives 1 and 2)
Coring program:	See text
Downhole measurements program:	Triple combo tool string, FMS-sonic, VSP
Nature of rock anticipated:	Muds, muddy sands, marls

Site GUB-03A

Priority:	Alternate
Position:	36.700975°N, 7.411174°W
Water depth (m):	540
Target drilling depth (mbsf):	1650
Approved maximum penetration (mbsf):	930 (Currently seeking EPSP approval for the full target drilling depth)
Survey coverage (track map; seismic profile):	Inline: GulfofCadiz_IL3260_GUB03A.sgy Position: CDP CDP888 Crossline: GulfofCadiz_XL2072_GUB03A.sgy Position: CDP CDP2279
Objectives:	• Recover a complete Late Miocene succession in the pathway of Mediterranean overflow • Obtain a high-resolution (precessional) record of Miocene Mediterranean overflow at an intermediate site between the onshore records (RIF-01A and BET-01A) and the distal record (ALM-03A) (Objectives 1, 2 and 3)
Coring program:	See text
Downhole measurements program:	Triple combo tool string, FMS-sonic, VSP
Nature of rock anticipated:	Muds, muddy sands, marls, sands

Site EAB-02A

Priority:	Alternate
Position:	35.75518251°N, 2.43956525°W
Water depth (m):	845
Target drilling depth (mbsf):	1277
Approved maximum penetration (mbsf):	1277
Survey coverage (track map; seismic profile):	Inline: GBT02 Position: SP 1955 Crossline: MSB12 Position: SP 1457
Objectives:	• Recover one of the few thick Late Messinian sedimentary successions in the Alboran Basin • Obtain key contraints on the chemistry and physical properties of Mediterranean overflow during the Late Miocene (Objectives 1, 2 and 3)
Coring program:	See text
Downhole measurements program:	Triple combo tool string, FMS-sonic, VSP
Nature of rock anticipated:	Marls, silts, sands and clays

Site EAB-03A

Priority:	Alternate
Position:	35.750427°N, 2.431305°W
Water depth (m):	838
Target drilling depth (mbsf):	1277
Approved maximum penetration (mbsf):	1277
Survey coverage (track map; seismic profile):	Inline: GBT02 Position: SP 2004 Crossline: MSB12 Position: SP 1432
Objectives:	• Recover one of the few thick Late Messinian sedimentary successions in the Alboran Basin • Obtain key contraints on the chemistry and physical properties of Mediterranean overflow during the Late Miocene (Objectives 1, 2 and 3)
Coring program:	See text
Downhole measurements program:	Triple combo tool string, FMS-sonic, VSP
Nature of rock anticipated:	Marls, silts, sands and clays

Site U1385/SHACK-04C (drilled to 400 mbsf on Expedition 397)

Priority:	Alternate
Position:	37°34.0002′N; 10°7.6644′W
Water depth (m):	2585
Target drilling depth (mbsf):	873
Approved maximum penetration (mbsf):	400; request to deepen to 873 mbsf pending at EPSP.
Survey coverage (track map; seismic profile):	Common midpoint (CMP) 1325 on JC089 Line 9 CMP 662 on JC089 Line 13 (nearest crossing)
Objective(s):	• Recover Late Miocene to Early Pliocene precessional-scale stratigraphy below 400 mbsf, the depth reached at this site on Expedition 397. • Obtain key contraints on the chemistry and physical properties of Mediterranean overflow during the Late Miocene (Objectives 1, 2 and 3).
Coring program:	1 hole: XCB to 400 mbsf; PDC bit
Downhole measurements program:	Triple combo tool string, FMS-sonic, VSP
Nature of rock anticipated:	Hemipelagic sediments